Acetylated cashew gum and fucan for incorporation of lycopene rich extract from red guava (Psidium guajava L.) in nanostructured systems: Antioxidant and antitumor capacity

Eryka Oliveira de Andrades, João Marcos Antônio Rodrigues da Costa, Francisco Edmar Moreira de Lima Neto, Alyne Rodrigues de Araujo, Fabio de Oliveira Silva Ribeiro, Andreanne Gomes Vasconcelos, Antônia Carla de Jesus Oliveira, José Lamartine Soares Sobrinho, Miguel Peixoto de Almeida, Ana P. Carvalho, Jhones Nascimento Dias, Ingrid Gracielle Martins Silva, Patrícia Albuquerque, Ildinete Silva Pereira, Doralina do Amaral Rabello, Adriany das Graças Nascimento Amorim, José Roberto de Souza de Almeida Leite, Durcilene Alves da Silva

PII: S0141-8130(21)02044-4

DOI: https://doi.org/10.1016/j.ijbiomac.2021.09.116

Reference: BIOMAC 19415

To appear in: *International Journal of Biological Macromolecules*

Received date: 10 June 2021

Revised date: 9 September 2021

Accepted date: 17 September 2021

Please cite this article as: E.O. de Andrades, J.M.A.R. da Costa, F.E.M. de Lima Neto, et al., Acetylated cashew gum and fucan for incorporation of lycopene rich extract from red guava (Psidium guajava L.) in nanostructured systems: Antioxidant and antitumor capacity, *International Journal of Biological Macromolecules* (2018), https://doi.org/10.1016/j.ijbiomac.2021.09.116

process, errors may be discovered which could affect the content, and all legal disclaimers that apply to the journal pertain.

Acetylated cashew gum and fucan for incorporation of lycopene rich extract from red guava (*Psidium guajava* L.) in nanostructured systems: Antioxidant and antitumor capacity

Eryka Oliveira de Andrades[a,b], João Marcos Antônio Rodrigues da Costa[b]; Francisco Edmar Moreira de Lima Neto[b]; Alyne Rodrigues de Araujo[b]; Fabio de Oliveira Silva Ribeiro[b]; Andreanne Gomes Vasconcelos[c]; Antônia Carla de Jesus Oliveira[d]; José Lamartine Soares Sobrinho[d]; Miguel Peixoto de Almeida[e]; Ana P. Carvalho[f,g]; Jhones Nascimento Dias[h]; Ingrid Gracielle Martins Silva[i], Patrícia Albuquerque[h], Ildinete Silva Pereira[h], Doralina do Amaral Rabello[j], Adriany das Graças Nascimento Amorim[b], José Roberto de Souza de Almeida Leite[b,c]; Durcilene Alves da Silva*[,a,b]

[a] Programa de Pós-Graduação em Biotecnologia, RENORBIO, Brazil;

[b] Núcleo de Pesquisa em Biodiversidade e Biotecnologia, BIOTEC, Universidade Federal do Delta do Parnaíba, UFDPar, Parnaíba, PI, Brazil;

[c] Núcleo de Pesquisa em Morfologia e Imunologia Aplicada, NuPMIA, Área de Morfologia, Faculdade de Medicina, Universidade de Brasília, UnB, Brasília, DF, Brazil;

[d] Núcleo de Controle de Qualidade de Medicamentos e Correlatos, NCQMC, Departamento de Ciências Farmacêuticas, Universidade Federal de Pernambuco, UFPE, Recife, PE, Brasil;

[e] LAQV/REQUIMTE, Departamento de Química e Bioquímica, Faculdade de Ciências, Universidade do Porto, Porto, Portugal;

[f] LAQV/REQUIMTE–GRAQ, Instituto Superior de Engenharia, Instituto Politécnico do Porto, Porto, Portugal;

[g] Centro de Biotecnologia e Química Fina, CBQF, Escola Superior de Biotecnologia, Universidade Catolica Portuguesa, Porto, Portugal;

[h] Laboratório de Biologia Molecular de Fungos Patogênicos, Instituto de Biologia, Universidade de Brasília, UnB, Brasília, DF, Brazil.

[i] Laboratório de Microscopia e Microanálise, Instituto de Biologia, Universidade de Brasília, UnB, Brasília, DF Brazil;

[j] Laboratório de Patologia Molecular do Câncer, Área de Patologia, Faculdade de Medicina, Universidade de Brasília, UnB, Brasília, DF, Brazil.

*Corresponding author: Durcilene Alves da Silva, PhD. Center for Biodiversity Research and Biotechnology (BIOTEC), Federal University of Delta of Parnaiba, Piauí. Avenue São Sebastião, CEP 64202-020. Phone: +55 86 33235433. Email:durcileneas@gmail.com

Abstract

Industrial application of lycopene is limited due to its chemical instability and low bioavailability. This study proposes the development of fucan-coated acetylated cashew gum nanoparticles (NFGa) and acetylated cashew gum nanoparticles (NGa) for incorporation of the lycopene-rich extract from red guava (LEG). Size, polydispersity, zeta potential, nanoparticles concentration, encapsulation efficiency, transmission electron microscopy (TEM) and atomic force microscopy (AFM) were used to characterize nanoparticles. The antioxidant activity was determinated and cell viability was evaluated in the human breast cancer cells (MCF-7) and human keratinocytes (HaCaT) by MTT assay. The toxic effect was evaluated by hemolysis test and by *Galleria mellonella* model. NFGa showed higher stability than NGa, having a size of 162.10±3.21 nm, polydispersity of 0.348±0.019, zeta potential -30.70±0.53 mV, concentration of 6.4×10^9 nanoparticles/mL and 60% LEG encapsulation. Microscopic analysis revealed a spherical and smooth shape of NFGa. NFGa showed antioxidant capacity by ABTS method and ORAC assay. The NFGa presented significant cytotoxicity against MCF-7 from the lowest concentration tested (6.25-200 µg/mL) and did not affect the cell viability of the HaCaT. NFGa showed non-toxic effect in the *in vitro* and *in vivo* models. Therefore, NFGa may have a promising application in LEG stabilization for antioxidant and antitumor purposes.

Keywords: lycopene; polysaccharides; nanoparticles; biocompatibility; antioxidant; antitumor.

1. Introduction

The *Psidium guajava* L. is a plant of great economic importance due to the commercialization of its fruit, the red pulp guava. Among the carotenoids present in the reddish pulp of the fruit, we highlight the lycopene, the content of which in the fruit in natura, as well as in its industrial derivatives, is higher in relation to watermelon, pitanga, papaya and tomato itself, which currently the main source of lycopene in developed countries [1]. Carotenoids can be extracted from different plant sources (leaves, bark, seeds, fruits, roots) and are cited in several epidemiological studies because they present as natural antioxidants [2,3], antifungal [4], antibacterials [5,6], anti-inflammatory [7], antitumor [8,9]. Carotenoids have benefits for mental health and metabolism, in adults (including pregnant women) and even children. The literature also demonstrates the application of these molecules in cosmetics, mainly due to their antioxidant potential [10].

Among the carotenoids, lycopene is considered a potent antioxidant, since it has the ability to react with free radicals, mainly singlet oxygen, formed from the irradiation of oxygen by ultraviolet (UV) rays, which is responsible for lipid peroxidation in cell

membranes [11,12]. In addition to the antioxidant activity, anti-inflammatory activity [13,14]; antifungal activity [15,16], cardioprotective activity [17,18] and neuroprotective activity [19,20] is attributed to lycopene. The antitumor activity is reported in several studies, with a great prominence under prostate cancer [21], ovary [22] and breast [23,24].

Chemically, lycopene is a hydrocarbon composed of a symmetric and acyclic structure containing 11 conjugated double bonds and 2 unconjugated bonds, this being the efficacy in the stabilization of singlet oxygen [25,26]. This chemical characteristic limits the use of lycopene in formulations, since the molecule is unstable to the presence of light, oxygen, heat and presents low bioavailability due to its hydrophobic nature [27].

The compound encapsulation in inclusion complexes, nanodispersions, nanoparticles, nanoemulsions, liposomes presents a perspective of improving physico-chemical characteristics, as well as the pharmacological and therapeutical efficacy. Using nanocarriers, several studies indicate promising results in the stability optimization of lycopene with increase of biological activity, well as to improve bioavailability [28-30].

Polymeric nanoparticles are often defined as solid colloidal particles having size in the range of 10-1000 nm [31]. These transport systems offer a great advantage over the others because their physicochemical properties can be controlled according to the composition of the polymers and the constituents of the nanoformulations [32,33]. Due to its ability to accommodate drugs of different levels of hydrophobicity, molecular weight and charge, polymeric nanocarriers are employed for various biological activities like anti-inflammatory, antiulcerogenic, hepatoprotectant and as intended in this study, antitumor and antioxidant [34-36].

In the present study, a lycopene-rich extract (LEG) was obtained from the red guava and was incorpored into a polymeric blend nanoparticle of modified cashew gum and fucan. The physico-chemical characterization, antioxidant activity and biological studies to evaluate biocompatibility and antitumor activity were performed.

2. Materials and methods

2.1. Chemicals and reagents

Ethanol, chloroform, acetone, Polysorbate 80, pyridine, formamide, acetylic anhydride were purchased from Dinâmica® Química Contemporânea Ltda (Brazil). Lycopene ≥90%, from tomato, penicillin and streptomycin, MTT (3-[4,5-dimethylthiazol-2-yl]-2,5 phenyltetrazolium bromide), ABTS (2,2′-Azino-bis(3-ethylbenzothiazoline-6-sulfonic acid), sodium fluorescein and AAPH (2,2′-Azobis (2-amidinopropane) dihydrochloride) were obtained from Sigma–Aldrich (Madrid, Spain). Dulbecco's modified Eagle's medium

(DMEM, Gibco BRL, USA) was used to cell culture. Acetonitrile and methanol (HPLC-grade) were purchased from Merck (Germany). N-hexane and ammonium acetate (HPLC-grade) were supplied by Tedia Company Inc. (USA) and J.T. Baker (Mexico), dichloromethane analytical grade from purchased Sharlab S.L (Spain).

2.2. Production and characterization of lycopene-rich extract from red guava (LEG)

The red guava was purchased in the local market, in the city of Parnaíba, state of Piauí, Brazil. The production of LEG was carried out in accordance with the methodology described in the patent n° EP2018017165320180509 by Amorim et al.[37]. The extract was dried on an evaporator route (Evaporator Route R-215, Buchi, Switzerland) at 175 mbar at room temperature. The LEG was analyzed by UV-Vis spectrophotometer (Shimadzu UV-1800, Japan) by scanning in the region of wavelength (λ) between 300 and 650 nm according to dos Santos et al. [38]. The quantification of lycopene in the extract was estimated at λ_{max} 472 nm from the all-*trans*-lycopene standard calibration curve. HPLC analysis of the LEG was conducted in consonance with Amorim et al. [39] using a Shimadzu liquid chromatographer (Japan), RPAQUEOUS Develosil-C30 analytical column (4.6 × 150 mm, 5 µm), mobile phase composed by acetonitrile, methanol, hexane, dichloromethane, ammonium acetate (55:22:11.5:11.5:0.02, v:v:v:v:w) at a flow rate of 1 mL/minute and UV-Vis detection between 800 and 200 nm at 1.2 nm/s with monitoring at 472 nm.

2.3. Obtaining acetylated cashew gum (CGa) and fucan (FUC) polysaccharides

Cashew gum (CG) was isolated from exudates from trees of the genus *Anacardium occidentale* L. native to Parnaíba, Piauí, Brazil. The extraction method followed the methodology described by De Paula, Heatley, and Budd [40] and Araújo et al. [41]. CG was modified by insertion of acetyl groupings (CGa) using acetic anhydride according to the methodology proposed by Pitombeira et al. [42]. Fucan (FUC) was obtained from the seaweed *Padina gymnospora* (Kützing) Sonder collected at Coqueiro beach, Luiz Correia - PI, Brazil and the extraction process was carried out according to Wang and Chen [43], with modifications. The dry mass of seaweed (10 g) was ground and hydrated in 1:20 (w/v) deionized water and heated (80 ± 5 °C) for 60 minutes under constant stirring. Then, the solution was filtered and adjusted to pH 7.0. For polysaccharide precipitation 1:3 (v/v) ethanol was added and the precipitate was then filtered and washed with acetone and subjected to hot air flow to obtain the dry mass of FUC.

2.4. Encapsulation of LEG in polymer carriers

2.4.1 Synthesis of fucan-uncoated acetylated cashew gum nanopartciles (NGa)

An polymer nanoparticle based on acetylated cashew gum and without fucan loading LEG, named NGa, was produced by nanoprecipitation method, in accordance with described by Gharib and Faezizadeh [44], with modifications. The organic phase was prepared by dissolving the LEG (10 mg) and CGa (10 mg) in acetone (5 mL) under magnetic stirring for 5 min. The aqueous phase, consisting of distilled water (5.3 mL) and tween 80 (7 mg for NGa1 and 14 mg for NGa2), was prepared under the same homogenization conditions as the organic phase. Then, the organic phase was slowly dripped into the aqueous phase under high shear homogenization (T 10 basic Ultra-Turrax®-Ika) at 15,000 rpm for 5 min. The residual organic solvent was removed in a vacuum concentrator (Eppendorf™ Concentrator Plus/Vacufuge®). NGa without LEG was produced as a blank control under the same synthetic conditions and was identified as NBGa.

2.4.2. Synthesis of fucan-coated acetylated cashew gum nanoparticles (NFGa)

An polymer nanoparticle based on acetylated cashew gum and fucan loading LEG, named NFGa, was produced according to the methodology detailed by Li et al. [45], with adaptations. The organic phase was prepared by dissolving the LEG (10 mg) and CGa (10 mg) in acetone (5 mL) under magnetic stirring for 5 min. The aqueous phase, consisting of distilled water (5.3 mL) and tween 80 (35 mg), was prepared under the same homogenization conditions as the organic phase. Then, the organic phase was slowly dripped into the aqueous phase in an ice water bath (4-8 °C) under high shear homogenization (T 10 basic Ultra-Turrax®-Ika) at 15,000 rpm for 5 min. Subsequently, the nanoparticles previously prepared were poured into the distilled water (7.5 mL) containing FUC (10 mg), under high shear homogenization (T 10 basic Ultra-Turrax®-Ika) at 15,000 rpm for 5 min. The residual organic solvent was removed in a vacuum concentrator (Eppendorf™ Concentrator Plus /Vacufuge®). NFGa without LEG was produced as a blank control under the same conditions and was identified as NBFGa.

2.5. Characterization of the nanoparticles

The mean particle size (z-average), polydispersity index (PDI) and zeta potential were determinated by Dynamic Light Scattering (DLS) using a Malvern Zetasizer Nano ZS90 equipment. The nanoparticles absorption spectrum was obtained using a UV-Vis spectrophotometer (Shimadzu UV-1800, Japan) by scanning in the region of wavelength (λ) between 350 to 650 nm. The concentrantion of nanoparticles and mean particle size was evaluated by Nanoparticle Tracking Analysis (NTA) using Malvern Panalytical NanoSight NS300 equipment with a 642 nm laser module (Malvern, UK) and NTA 3.3 software. For morphological analysis were employed Atomic Force Microscopy (AFM) using a TT-AFM

(AFM Workshop, USA) in vibrating mode and Transmission Electron Microscopy (TEM) using a JEOL JEM-1011 at 10 kV with 20 mm aperture.

2.6. Encapsulation efficiency

The encapsulation efficiency was measured according to Li et al. [43] with modifications. Nanoparticles solutions were diluted in chloroform: ethanol (2:1, v:v) at the ratio of 1:2 (v:v), vortexed for 10 minutes and then centrifuged at 15,000 rpm for 15 minutes. The supernatant was removed and the precipitate containing LEG was analyzed using a Shimadzu UV-1800 spectrophotometer (Japan) by scanning in the region of wavelength (λ) between 300 to 650 nm. This procedure was also performed using nanoparticles without LEG as a blank solution. The quantification was performed at 472 nm and the encapsulation efficiency (EI) was calculated by equation below:

$$\%EE = Me / Mi \times 100 \quad \text{(Eq. 1)}$$

Where Me is the mass of LEG quantified in the precipitate and Mi is the initial mass of LEG added in the system.

2.7. Stability study of the nanoparticles

To evaluate the colloidal stability of the nanoparticles and the nanoencapsulated LEG stability, the samples were stored under refrigeration (4 °C) and room temperature (27 °C). The mean particle size, PDI, zeta potential and pH were analyzed monthly over 90 days. The stability of LEG encapsulated in the nanoparticles was evaluated through the absorption spectrum using a UV-Vis spectrophotometer (Shimadzu UV-1800, Tokyo-Japan) by scanning in the region of wavelength (λ) between 300 to 650 nm. The quantification of lycopene equivalent was performed on the day of synthesis (day 0) and after 90 days. Free LEG was evaluated under the same conditions of analysis and storage as control.

2.8. Fourier transform infrared spectroscopy (FTIR)

Infrared absorption spectrum of the LEG, CG, CGa, FUC, NBFGa and NFGa were measured using the IRAffinity-1S (Shimadzu, Japan) equipment. Infrared spectra were recorded at the range from 4000 to 700 cm^{-1} in transmittance mode.

2.9. Antioxidant activity

The antioxidant activity of the NFGA was evaluated by the ABTS colorimetric method, according to Okonogi and Riangjanapatee [30]. The absorbances were measured in a spectrophotometer at 750 nm after 6 min of reaction. The calibration curve of the Trolox synthetic antioxidant standard was prepared varying the concentrations from 7.8 to 125 μM e the results were expressed TEAC (Trolox μM equivalent antioxidant capacity).

The oxygen radical absorbance capacity (ORAC) assay was performed as described by Mendes et al. [46]. Measurements were performed on Multi-mode Microplate Reader (BioTek Instruments, USA). The calibration curve was obtained with Trolox in dilutions between 12.5 and 100 μM and expressed at TEAC (Trolox μM equivalent antioxidant capacity).

2.10. Biological studies

2.10.1. Cell culture

Human breast adenocarcinoma (MCF-7) and human keratinocyte (HaCaT) cell lines were obtained from the American Type Culture Collection (ATCC®, USA). Cells were cultured in Dulbecco's modified Eagle's medium (DMEM) supplemented with 10% fetal bovine serum (Gibco, USA) and 1% antibiotic solution (10 000 IU/mL penicillin and 10 mg/mL streptomycin, in a humid atmosphere at 37 °C and 5% CO_2.

2.10.2. Cell viability assay

The cell viability assay was performed by the MTT dye reduction method as described by Vasconcelos et al. [47]. MCF-7 and HaCaT cells were seeded at a density of 3 x 10^3 into 96-well plate in DMEM culture medium and incubated for 24 hours at 37 °C in a CO_2 incubator. The cells were treated with NFGa, NBFGa diluted in DMEM and LEG diluted in 0.5% DMSO at a concentration range from 6.25 to 200 μg/mL. Cells were incubated for 24 and 72 hours at 37°C and 5% CO_2. DMEM and 0.5% DMSO were used as cell viability control. After exposure time, the supernatant was discarded and 150 μL of DMEM containing MTT at 5 mg/mL was added in each well, following incubation for 2 hours at 37 °C and 5% CO_2. Thereafter, the supernatant was removed and 100 μL of DMSO was added to dissolve the blue formazan crystals produced from the metabolism of MTT by living cells. The absorbance was monitored at 595 nm using a SpectraMax® Plus 384 plate reader (Molecular Devices, USA). The tests were performed in quintuplicates in two independent experiments.

2.10.3. Hemolytic activity

Hemolytic activity was evaluated according to dos Santos et al. [38]. A volume of 4 mL of sheep (*Ovis aries*) blood was collected in tubes containing EDTA (1.8 mg/mL). The animal is from the Água Limpa Farm of the University of Brasília-UnB, Brazil. The experiment was approved by Animals Ethics Committee of the Institute of Biological Sciences of the University of Brasília under protocol number 09/2019. The blood was washed with phosphate-buffered saline (PBS) and a 5% erythrocytes solution was prepared. NFGa and NBFGa diluted in PBS was added (20 μL) to cell solution (80 μL) into a 96-well plate. The samples were tested at a concentration range from 6.25 to 200 μg/mL. After incuation for 1 hour at a 37 ºC the reaction was interrupted and the samples were centrifuged at 3,000 rpm for

10 minutes. The supernatant was measured at 550 nm using a SpectraMax® Plus 384 plate reader (Molecular Devices, USA). PBS (1x) was used as the negative control and Triton-X (0.1% v/v) was used as the positive control. The percentage of hemolytic activity was calculated by the following equation:

$$\%HA = \frac{ABSsample - ABSsaline}{ABStriton - ABSsaline} \times 100 \quad \text{(Eq. 2)}$$

Where ABS is the absorbance value.

2.10.4. In vivo toxicity in the *Galleria mellonella* model

The toxicological evaluation in the *Galleria mellonela* model was performed according to Ignasiak and Maxwell [48] and do Nascimento Dias et al. [49]. Groups containing sixteen sixth instar larvae (250-300 mg) received injections of 10 uL of different doses of NFGa (5, 10 and 20 mg/kg). The control group received only PBS. The larvae were incubated at 37 ºC for seven days with daily monitoring of deaths. The analysis were carried out in two independent experiments.

2.11. Statistical Analysis

The statistical analysis of the nanoparticles characterization data (size, PDI, zeta Potential and encapsulation efficiency) was carried out by one-way ANOVA followed by Tukey post-test. Cell viability data were evaluated by analysis of variance (ANOVA) followed by Bonferron's multiple comparison test to verify statistical differences between groups. Two-way ANOVA followed by Bonferroni's multiple comparison analyses were employed to compare means between the exposure times 24 and 72 h. Log-rank was used in the analysis of Mantel-Cox survival curves. All analyzes were performed using GraphPad Prism 6.0 (GraphPad Softwares, USA) and the results expressed as mean ± standard error of the mean (SEM). The statistical significance was set at $p < 0.05$.

3. Results and Discussion

3.1. Characterization of LEG by UV-Vis spectrophotometry and HPLC-DAD

The UV-Vis spectrum of lycopene standard (LS) and lycopene-rich extract from red guava (LEG) in ethanol are shown in Fig. 1A. The spectrum obtained with scanning between 650-300 nm show that the LEG absorbance pattern is similar to the LS absorbance pattern, with wavelength of maximum absorbance (λmax) of 446, 472 and 504 nm. This data corroborate with the UV Vis spectrum of the lycopene-rich extract from tomato [50, 51], as well as to the LEG previously described by Santos et al. [38]. The lycopene content in the extract was 34.4% per dry mass. The concentration of lycopene in the extract may vary due to

its own lycopene content in fruits and vegetables related to climatic and edaphic variables, stage of maturation, planting of varieties, postharvest, management and storage [52].

Comparing the LS with the LEG chromatogram, the same retention time (RT = 9.36 minutes) is observed (Fig. 1B). In the LEG chromatogram there are also two other peaks at 8.75 and 15.34 minutes. These results are similar to the chromatogram of the lycopene-rich extract from red guava obtained by [36] where it presents the same retention time corresponding to the lycopene standard (RT = 10.5 minutes) and two other peaks at different retention times (RT = 9.5 and 16.1 minutes), which wereattributed to the presence of other carotenoids.

3.2. Characterization of polymer nanoparticles

In this study, two natural polymers were explored for production of nanoparticles loading LEG: acetylated cashew gum and fucan, a sulfated polysaccharide from seaweed. The acetylation of the cashew gum (CG) was promoted through the reaction with acetic anhydride (Fig. 2). The chemical modification is usually carried out with the primary hydroxyl group (C6) of the sugar due to the greater reactivity of this position in relation to the secondary or tertiary portions [53]. The replacement of numerous hydrophilic hydroxyl groups as a result of the insertion of acetyl groups in the polymeric chain of CG promotes changes in the solubility of the gum, making it insoluble in water. Thus, through the process of nanoprecipation, when the organic phase containing a mixture of acetone, LEG and CGa is dispersed under an aqueous phase allows the assembly of a self-organized system [42].

Table 1 presents composition and characterization data of polymeric nanoparticles loading LEG and without the extract (blank control). It is possible to observe that the size of NBGa (189.3 ± 0.4 nm) was significantly lower ($p < 0.05$) than NGa1 and NGa2, probably due incorporation of LEG. The PDI (0.25 ± 0.02) and zeta potential (-26.5 ± 1.1 mV) of NBGa was significantly higher ($p < 0.05$) than NGa1 and NGa2. The differences on the particle size, PDI, zeta potential and encapsulation efficiency were also observed between NGa1 and NGa2. NGa2 presented size and PDI significantly larger ($p < 0.05$) than NGa1 as opposed to the zeta potential that was significantly lower ($p < 0.05$). The variation in these parameters may be due to the increased surfactant concentration.

Sharma, Madan, and Lin [54] in a study that aimed to evaluate the effect of process and formulation variables on the synthesis of nanoparticles from biodegradable polymers for the carrying of paclitaxel noted that as increased concentration of the surfactant poly-vinyl alcohol (PVA) at 0.10; 0.25; 0.50; 0.75; 1.0 and 2.0%, the particle size and PDI increased, while the encapsulation efficiency decreased when the higher concentrations are used (0.75;

1.0 and 2.0%). According to the authors, the effect of the surfactant concentration on these parameters could be explained by the gelatinization of PVA molecules due to the strong hydrogen bonds via the hydroxyl group, thus the gelatinization of PVA at the oil/water interface can occur during the formation process of nanoparticles.

Kheradmandnia et al. [55] synthesized lipid nanoparticles for incorporation of ketoprofen using a combination of lectin and tween 80 as surfactants, the latter being used in the formulation at concentrations of 40; 50; 60 and 100%. In the formulation where the concentration of tween 80 was 100%, there was an increase in particle size and PDI and the zeta potential showed a proportional decrease as the tween 80 concentration was increased, reaching the lowest value (-8.60 mV) when 100% tween 80.

About fucan-coated acetylated cashew gum nanoparticles (Table 1), the nanoparticles without LEG (NBFGa) showed a size and PDI significantly larger ($p < 0.05$) than nanoparticles containing LEG (NFGa), however, there was no significant difference in the zeta potential of NBFGa compared to NFGa.

Previous studies using acetylated cashew gum as a polymer for the incorporation of hydrophobic active compounds presented similar behavior regarding particle size when incorporated into the active. Rodrigues et al. [56] synthesized nanoparticles with acetylated cashew gum for the incorporation of epiisopiloturin, a slightly water soluble alkaloid, the incorporation of the active in the polymer matrix significantly reduces the particle size, as did studies developed by Pitombeira et al. [42] that when synthesizing nanoparticles using acetylated cashew gum to incorporate indomethacin, hydrophobic compounds, the nanoparticles without indomethacin incorporated showed larger sizes than the nanoparticles incorporated with the active.

In general, in relation to the size of the nanoparticles, NBGa had a smaller average size ($p < 0.05$) than NGa1 and NGa2, in contrast to NBFGa, whose average size was larger ($p < 0.05$) than NFGa. It is worth mentioning that NFGa has the smallest size and NGa2 the largest among the nanoparticles produced in the study ($p < 0.05$). NFGa did not show significant difference in the zeta potential when compared to NBFGa, however, NBFGa and NFGa showed zeta potential greater than NBGa, NGa1 and NGa2 ($p < 0.05$).

Several parameters in the synthesis can influence the characteristics of the nanoparticles and using the nanoprecipitation method the main aspects that seem to have influenced the size, PDI, zeta potential and encapsulation efficiency of the nanoparticles synthesized in this study were the nature and concentration of the polymers, concentration of active and surfactant in the reaction medium [57].

The biological application of loading systems depends in part on the particle size. Banerjee et al. [58] affirmed that nanoparticles with a diameter in the range of 50 nm to 200 nm are better absorbed and transported by intestinal cells more efficiently when compared to larger particles because these reduced sizes provide higher solubility, reactivity and efficiency to deliver bioactive compounds in the gastrointestinal tract, as well as facilitate penetration into biological barriers. Danaei et al. [59] points out that nanovesicles with a diameter of 300 nm or below can distribute their content to some extent in the deeper layers of the skin, particles in the 10-210 nm size range may preferentially penetrate the transfollicular pathway. In the present study, the nanoparticles produced present satisfactory scale sizes for a nanocarrier for the pharmaceutical, food and cosmetic industries.

The PDI is a representation of the particle size variability in a colloidal system that may eventually arise as a result of factors associated with the synthesis process [60]. The degree of polydispersity is measured in a distribution range consisting of the value of 0.0 (system with uniform particle size) to 1.0 (polydispersed system with populations of particle size). Within this range, the polydispersity index of 0.3 indicates a narrow particle size distribution. In this study, the PDI values presented by the nanoparticles correspond to a system with relatively uniform distribution [61].

The zeta potential is used to determine the surface charge and stability of a colloidal suspension and considered to be indicative of good colloidal stability. According to DLVO theory, zeta potential values in modules between 0 mV and 10 mV demonstrate highly unstable particles, 10 mV at 20 mV relatively stable particles, 20 mV at 30 mV moderately stable and values above 30 mV highly stable particles [58,62]. The surface charge values of NGa1 and NGa2 confer a relative stability to the colloidal system and we infer that although the hydroxyl groups of Tween 80 can contribute slightly to the negative charge, even in the case of a nonionic surfactant, the charge of the zeta potential is attribution mainly to the acetyl groups inserted in the CG. The surface load values of NFGa are consistent with a system of high stability and the negative value is related, in addition to the acetyl groups inserted in the cashew gum or Tween 80, with the sulphate groups of the fucana. Thus, stabilization in suspension can occur from electrostatic force (polysaccharide loading) and steric (by surfactant) [56,61,63].

The Fig. 3 shows the absorption spectrum of the nanoparticles after synthesis (day 0). The UV-Vis spectrum of NBGa (Fig. 3A) and NBFGa (Fig. 3D) showed absence of LEG absorption profile, while the UV-Vis spectrum of the nanoparticles containing LEG (Fig. 3B, C and E) presents characteristic lycopene absorption bands. When comparing the UV-Vis

spectrum of NGa1, NGa2 and NFGa (Fig. 3B, C and E, respectively), the maximum wavelengths of the LEG were more evident in the NGa1 and NGa2 spectra. These suggest that the LEG may have adsorbed in the polymeric matrix, which may be the reason why the extract was not adequately protected from possible chemical degradation, as there was a gradual decrease in the maximum wavelengths of the LEG in the NGa1 and NGa2 spectrum to the point that they are no longer evident at the end of a month of synthesis. In addition, this fact may have contributed to a low encapsulation efficiency in both nanoparticles (Table 1). The UV-Vis spectrum of NFGa shows more subtle maximum wavelengths of the LEG, suggesting that the FUC coating for CGa nanoparticles containing LEG was efficient, reflecting an improvement in the system and increasing the efficiency of the encapsulation (Table 1).

Temporal colloidal stability under different storage conditions is a challenge and several factors can affect the stability of nanoparticles in suspensions during the storage period. The stability test in this study was performed by storing the nanoparticles in refrigeration (4 °C) and room temperature (~27 °C) in a period of 90 days. Size, PDI, zeta potential and pH values are shown in Table 2. At room temperature, all nanoformulations showed degradation profile around 30 days, with precipitation of nanoparticles and phase separation. At 4 °C, NGa1 and NGa2 in the second month exhibited degradation profile (precipitation and phase separation), while NFGa showed no significant difference in size ($F = 0.899$, $p = 0.456$), PDI ($F = 0.270$, $p = 0.772$), zeta potential ($F = 2,430$, $p = 0.169$) and pH ($F = 2,275$, $p = 0.184$) when stored at 4 °C for periods of 90 days. After this time, the LEG extracted from the nanoparticles showed the same absorption spectrum as the first day, with three characteristic maximum absorption peaks, by UV-Vis technique (Figure S1).

Changes in particle size and PDI may be due to particle aggregation mediated by variation of zeta potential, pH, encapsulated active concentration, among others [57]. The pH changes suggest influence of this parameter in the nanoparticle stability, the pH decreased with increasing temperature, which may affect the polymeric matrix [57,64]. In addition to temperature and pH, the phase separation in nanoparticles suspensions is commonly related chemical composition of the nanoparticles [65, 66]. Thus, the presence of fucan in NFGa can contribute to stability. The behavior observed in the UV-Vis spectrum suggests that there was no degradation of lycopene, since lycopene degradation by reversible isomerization of all-trans lycopene to more oxidizable cis isomers promotes promotes changes in physical and chemical properties that are reflected in the UV-Vis spectrum [67,68].

During the stability study period, the LEG incorporated in the nanoparticles was evaluated and as a stability parameter, the free LEG was evaluated under the same storage conditions as the nanoparticles. According to the previous data presented in Table 2, the NFGa showed better stability and even after the 90 days of storage, there was no significant difference ($p = 0.253$) in the percentage of LEG incorporated. However, the free LEG, after 90 days at the same storage conditions, significantly decreased ($p < 0.05$) the lycopene content by 26%. In view of what has been reported so far, we conclude that NFGa nanoparticles at 4 ºC maintained the physico-chemical characteristics of the system, in addition to actually preserving the encapsulated LEG at a rate of 60%, therefore, it was the system selected for the continuation of this study.

The NFGa were evaluated by nanoparticle tracking analysis (NTA). This characterization technique combines dynamic light scattering and Brownian motion with laser light scattering microscopy with a coupled charge device (CCD) camera which allows individual particle analysis to obtain particle distribution and concentration through size *versus* counting in numbers. NTA is a technique that categorically represents a major advance for the study of polydispersed systems, because the main characterization technique used, DLS, is more sensitive to the presence of large particles, this is because the size of the particles is determined by fluctuations in the intensity of the scattered light. Due to the Brownian motion of the particles, thus it can lead to an inaccurate size determination in colloidal systems [65,69].

The NTA data (Fig. 4) revealed that the particles have a modal size of 125 nm with a concentration of 6.04 x 10^{12} nanoparticles/mL. The data obtained by NTA corroborate the data obtained by DLS, indicating a system with size distribution narrow.

The morphological characterization by microscopic techniques, in particular transmission electron microscopy (TEM) and probe scanning microscopy (AFM), have been the widely used methods to characterize nanometric materials [70].

TEM allows you to obtain images with a significantly higher resolution [71]. The investigation of the morphology of NBFGa (Fig. 5A) and NFGa (Fig. 5B) by TEM, demonstrate a particle size less than 200 nm with a spherical and smooth nature, in addition, it is possible to observe dark regions around the nanoparticles. Pereira et al. [72] when analyzing by TEM the morphology of PLGA nanoparticles for the incorporation of guabiroba extract rich in phenolic and carotenoid compounds attributed the shading at the edges of the nanoparticles to the suffactor, which forms connections between their hydrophobic regions with the polymeric chain, while its hydrophilic regions are exposed to the aqueous phase.

According to Tsapis [73] the surfactant can produce artifacts that are observed next to the nanoparticles. In some regions, it is also possible to observe slight aggregations of the nanoparticles, which is quite common, since the malleable walls of the polymeric particles can undergo forces of interfacial attraction during the evaporation of the solvent in the analysis substrate [74].

The smooth appearance and spherical shape of the nanoparticles by AFM corroborate the data obtained by TEM, as shown in Fig. 5C-D (NBFGa) and Fig. 5 E-F (NFGa). The average size for NBFGa was 173 ± 13.9 nm and for NFGa 125 ± 8.65 nm. The ability of the AFM to produce accurate results depends on several aspects such as how to sample preparation, type of substrate, resolution, software used, mode of operation of the instrument, measurement cantilever interaction, pixel size and scan rate [75]. In this study, in order to minimize the formation of aggregates and obtain reliable results, the methodology was carefully employed, considering the type of sample, the dilution and the type of material for the deposition of the sample.

In addition to the morphological aspect, it is possible to observe with the microscopic images of NBFGa and NFGa that there is a very homogeneous size distribution, therefore, there is a correlation with the data of medium size and polydispersion of nanoparticles obtained by DLS and NTA.

3.4. Fourier transform infrared spectroscopy (FTIR)

In order to characterize the most important organic groups referring to the components of the nanoparticles, analysis by Fourier transform infrared spectroscopy (FTIR) of the cashew gum (CG), acetylated cashew gum (CGa), fucan (FUC), lycopene-rich extract from red guava (LEG), NFGa and NBFGa (Fig. 6).

In the CG spectrum (Fig. 6A) it is possible to observe in 3340 cm^{-1} to stretching O-H; 2951 cm^{-1} and 2887 cm^{-1} symmetric and asymmetric stretching of C-H respectively; 1734 cm^{-1} axial deformation of C = O in COOH; 1373 cm^{-1} to stretching C = O; 1149 cm^{-1}, 1089 cm^{-1} and 1038 cm^{-1} are attributed to stretching C-O-C and O-H, referring to the glycosidic units [42,76]. Observing the CGa spectrum (Fig. 6A), there is a significant reduction of the band by 3380 cm^{-1} and an intensification of the bands of 1375 cm^{-1} and 1745 cm^{-1}, typical of the vibrational frequencies of carbonyl C = O, which can be attributed to acetylation. In addition, the corresponding bands 1149 cm^{-1}, 1089 cm^{-1} and 1038 cm^{-1} attributed to the C-O-C and O-H section referring to the glycosidic units appear as a single absorption peak [77,78].

In the FUC spectrum (Fig. 6A) the band at 3297 cm^{-1} is attributed to stretching O–H; 2883 cm^{-1} symmetric stretching of C-H; 1601 cm^{-1} and 1410 cm^{-1} asymmetric stretching to

COO of glucuronic acid and symmetric glucuronic acid vibrations respectively. The band at 1226 cm^{-1} and 1129 cm^{-1} are attributed to asymmetric stretching of S = O; 1080 cm^{-1} is due to the stretching of C-O-C relative to the glycosidic units [79-81].

In the LEG espectrum shown in Fig. 6B, the peak at the 994 cm^{-1} region is attributed to *trans* angular deformation outside the C-H plane; the bands at 1460 cm^{-1}, 1743 cm^{-1}, 2855 and 2927 cm^{-1} are respectively attributed the angular deformation C-H, the *trans* stretching of C = C; to the strong stretching for symmetrical methylene (CH sp^2) and asymmetric methyl (CH sp^3). The FTIR characterization of lycopene-rich extract from red guava showed vibrational frequencies similar to those of Priam et al. [82] and Santos et al. [38].

The NBFGa and NFGa absorption peaks (Fig. 6B) in the region of 1700 cm^{-1} and 1368 cm^{-1} can be attributed to a displacement respectively of the 1745 cm^{-1} and 1375 cm^{-1} regions present in the CGa spectrum. The vibrational frequency at 1427 cm^{-1} can be attributed to a displacement of the vibrational frequency in the region of 1410 cm^{-1} and the intensification at 1239 cm^{-1} can be attributed to the intensification of 1226 cm^{-1}, frequencies of functional groups present in the spectra of the FUC. The vibrational frequencies at 1093 cm^{-1} are attributed to the displacement of C-O-C present in both polysaccharides. These results suggest that there was an interaction of polysaccharides in the polymer mixtures for LEG encapsulation. Comparing the LEG spectrum with the NFGa spectrum (Fig. 6B), the disappearance of the characteristic peaks of the extract at 2927 cm^{-1}, 12855 cm^{-1}, 1460 cm^{-1} and 994 cm^{-1} indicates that there was an incorporation of the extract in the polymeric matrix. Nascimento et al. [83] characterized by FTIR polymeric nanoparticles based on PCL (polycaprolactone) for incorporation of red propolis extract. When comparing the absorption spectrum of empty nanoparticles and the nanoparticles loaded with the extract observed that both contained similar absorption peaks and when compared to the extract spectrum they observed the disappearance of characteristic peaks of the extract, thus suggesting the incorporation of the extract in the polymeric matrix.

Akhoond Zardini et al. [61] through analysis of FTIR spectra of lipid transporters for the incorporation of lycopene, observed that the transported and empty nanoparticles presented the same vibrating frequencies for both spectra and also suggested that the absence of new peaks in the spectra of the transported nanoparticles when compared to the spectra of the empty nanoparticles, they indicate that adsorption occurred in the lipid matrix.

3.5. Antioxidant activity

Due to the complexity of the sample, reaction mechanism and different reaction substrates, the correlation and comparison between the results against different trials to

evaluate antioxidant capacity becomes difficult, so there is a need to use of more than one method to infer the antioxidant capacity.

The antioxidant capacity of NFGa was evaluated by the ABTS and ORAC assays, both of which allow evaluating the antioxidant capacity of lipophilic or hydrophilic compounds. The ABTS assay is a colorimetric test based on the reaction with an organic cation ($ABTS^{\bullet+}$), while the ORAC assay is based on the decrease in fluorescence of phycobilin class proteins through the peroxyl radical reaction induced by AAPH (2,2'-azobis-2-amidinopropane). Because of the use of peroxyl radicals or prooxidant hydroxyls, the ORAC assay is very biologically relevant since it uses radicals similar to those occurring *in vivo* [84]. In Table 3 we find the results of the antioxidant activity of NFGa by the ABTS and ORAC assay expressed as TEAC (Trolox equivalent antioxidant activity).

Previous studies with a lycopene-rich extract from red guava showed TEAC values of 2980 ± 34 μM Trolox equivalent /g by ABTS method and 402.80 ± 44.40 μM Trolox equivalent/g by ORAC assay [36]. Additionally, nanoemulstion containing lycopene-purified from red guava presented TEAC of 127.66±0.45 μM Trolox equivalent/g [85]. In this context, the TEAC values of NFGa suggest a satisfactory antioxidant capacity.

From the preparation of solid lipid carriers with different concentrations of tomato extract (90% lycopene), Okonogi and Piangjanapatee [30] obtained different values of TEAC against the radical $ABTS^{\bullet+}$, with a TEAC value of 36.6 μM Trolox equivalent /mg for the nanocarrier with the maximum concentration of 50mg of lycopene, the TEAC values obtained were lower than that of this study using NFGawith lower concentration of incorporated LEG. Pereira et al. [86] encapsulated in polymer nanoparticles from PLGA guabiroba extract rich in phenolic compounds and the TEAC values against the ORAC assay was 229.0 μM Trolox equivalent/g.

3.6. Cell viability on human breast cancer cell and human keratinocytes

The viability assay was performed on human breast adenocarcinoma (MCF-7) and human keratinocyte normal cell line (HaCaT) lines exposed to LEG, NBFGa and NFGa at concentrations range from 6.25 to 200 μg/mL for 24 and 72 hours. Fig. 7 shows the cell viability in MCF-7 at 24 and 72 hours. Free LEG (Fig. 7A) there was a significant reduction ($p < 0.05$) in cell viability (24.35% of reduction) from 6.25 μg/mL, while for NBFGa the reduction in cell viability was significant from the 25 μg/mL (32.54% of reduction). However, there was a significant reduction ($p < 0.05$) in cell viability in all concentrations of NFGa, being able to observe a reduction of almost 41.24% in cellular viability at the lowest concentration (6.25 μg/mL). At 72 h (Fig. 7) the cytotoxic effects were significant ($p < 0.05$)

for all concentrations of free LEG, NBFGa and NFGa, with a reduction of 51.98%, 40.20% and 55.50% in cell viability at 6.25 μg/mL, respectively. Since the effect did not occur in dose-dependent manner, it not was possible to calculate the $IC_{50.}$ Statiscally significant difference was observed between exposure times of 24 and 72 hours for LEG, NBFGa and NFGa.

In a previous study with lycopene-rich extract from red guava in MCF-7, Santos et al. [38] observed that the viability reduction was time and dose dependent, exhibiting a cytotoxic effect for 24h treatment from the lowest concentration used (6.25 μg/mL; IC_{50}= 29.85 μg/mL). The cell viability was similar to the results in this work for LEG. Furthermore, the cytotoxic activity of LEG was optimized when nanoencapsulated, similarly to found by Vasconcelos et al. [47] for lipid-core nanocapsules containg LEG with a reduction of MCF-7 viability of 61.45% at 6.25 μg/mL at 24 hours of exposure.

The higher cytotoxic effect of nanoparticles loading LEG in relation to free LEG may be related to the form of cell uptake, since it is suggested that the absorption of lycopene occurs in a passive way mediated by proteins or added to lipid droplets, whereas the polymer nanoparticles are through an endocytic pathway, which may result in increased cellular uptake of the LEG in the encapsulated form [87,88].

Puri et al. [88] evaluated the cytotoxic effect of docetaxel-loaded polymer nanoparticles at 24, 48 and 72 hours in insensitive androgen-sensitive prostate cancer cell lines (PC3 and LNCaP, respectively). The nanoparticles had the spherical shape with a mean size of 265 ± 2 nm, PDI 0.23 ± 0.003 and zeta potential of -30.1 ± 0.5 mV, characteristics of particles similar to those obtained in this work. The docetaxel-loaded polymer nanoparticles showed a dose-time cytotoxic effect dependent more effectively on the same molar amount as the free drug, with the cell line LNCaP being more sensitive to docetaxel than PC3 cells. Akl et al. [89] evaluated the effect of curcumin-loaded PLGA polymer nanoparticles under the colon adenocarcinoma cell line (HT29 cells). The cytotoxic effect on the lineage studied was potentiated in comparison with free curcumin.

According to Fig. 8, the treatment of HaCaT non-cancerous cell line with free LEG did not significatively affect the viability at 24 hours of exposure. The reduction of the HaCaT viability was only at the highest concentration of NBFGa (200 μg/mL, 45.29% of reduction) and NFGa (100 and 200 μg/mL, 35.04% and 48.02% of reduction, respectively). At the 72 hours of exporure, the HaCaT viability was significantly ($p < 0.05$) affected by free LEG, NBFGa and NFGa from the 25 μg/mL.

These results suggest the anticancer potential of LEG encapsulated in the polymeric nanoparticles, because its cytotoxicity to cancer cells at low concentration and low cytotoxic effect to non-cancerous cells. In addition, several studies indicate that nanoparticles ≤ 200nm demonstrate efficiency in targeting tumor tissues through a passive mechanism that makes use of increased retention and permeability in tumors, called *enhanced permeability and retention effect* (RPE), and prevents rapid leakage in the blood capillaries, resulting in high antitumor efficacy potential [90,91].

3.7. Toxicity assessment

Erythrocytes are the most abundant blood cells and an *in vitro* toxicity test for hemolytic activity is a very effective test for assessing the biocompatibility effects of new biotechnological products [92,93]. The haemolytic activity test showed no cytotoxic effect of NFGa in sheep erythrocytes at the tested concentrations (6.25 to 200 μg/mL) (Fig. 9A). In an earlier study, Santos et al. [38] evaluated the hemolytic activity of lycopene-rich extract from red guava in sheep erythrocytes and showed a very slight reduction in cell viability (5%) at the highest concentration tested (800 μg/mL). Additionally, a lipid-core nanocpasule containing LEG does not affect the viability of sheep erythrocytes at concentration range from 6.25 to 200 μg/mL, corroborating our results [47]. These data indicate that polymeric nanoparticles loading LEG present biocompatibility with the normal cell model used.

Chiste et al. [94] evaluated through peroxyl radical toxicity ($ROO^{\bullet}$) the potential of carotenoids to inhibit hemolysis of human erythrocytes and lycopene was the most efficient to prevent hemolysis, followed by β-carotene, lutein and zeaxanthin. Our results showed biocompatibility even at the highest doses and seem to corroborate with the studies mentioned above, since lycopene is the carotenoid with the highest antioxidant activity moreover there are studies relating the sulfate polysaccharide (fucan) to a good antioxidant activity.

In vivo toxicity is a prerequisite for testing compounds for use in humans and tests on *G. melonella* larvae is an alternative to the cost, time and ethical criteria required for testing on mammals. The advantage of this cytotoxicity model is that the immune system of the *G. mellonella* larvae is similar in structure and function to the innate immune system of vertebrates, thus it is being established as a model for tests of infectivity and toxicity [48,95]. The *in vivo* test on *G. mellonella* larvae presents no toxic effect of NBFGa or NFGa at 5, 10 and 20 mg/kg (Fig. 9B), corroborating the hemolysis test. Spadari et al. [96], evaluated through the hemolysis and survival test of *G. mellonella* larvae, the effect of miltefosine encapsulation in alginate nanoparticles and the results showed that in addition to reducing the toxicity of miltefosine, the nanoparticles polymeric compounds showed low toxicity. In view

of the promising results, we suggest that the polymeric carrier in the present study is a safe formulation and the LEG carrier did not alter the biocompatibility of the system.

4. Conclusion

The fucan-coated nanoparticle obtained from modified cashew gums presented promising results for applicability in hydrophobic compounds carrying systems as lycopene-rich extract. The nanoparticles remained stable to the temporal degradation to which the extract is subject when free. In addition, the nanoparticles optimized the cytotoxic effect of free LEG on breast cancer cell, presented biocompatibility with human keratinocytes and sheep erythrocytes and was no toxic to *Galleria mellonella* larvae. Therefore, because it is a natural composition, these results suggest a potential complementary alternative for the treatment of the disease, since, chemotherapeutics present high dose cytotoxicity. We suggest more studies using additional biological models to expand the results.

Funding

To Coordenação de Aperfeiçoamento de Pessoal de Nível Superior - Brazil (CAPES) by support through Project number 1713871.

Acknowledgment

Laboratory of Advanced Materials, LIMAV, Federal University of Piauí, Teresina, PI on behalf of Profa. Dra. Carla Eiras for the concession in the use of equipment and materials assigned to the analyzes of DLS.

References

[1] Fredaa, S. A., Luvielmob, M. d. M., Rutza, J. K., & Zambiazi, R. C. (2018). Lycopene: effect of the heat treatment in the chemical structure and bioavailability. Estudos Tecnológicos em Engenharia, 12 ((2)), 23.

[2] Laus, M. N., Soccio, M., Giovannini, D., Caboni, E., Quacquarelli, I., Maltoni, M. L., Scossa, F., Condello, E., & Pastore, D. (2015). Assessment of antioxidant activity of carotenoidenriched extracts from peach fruits using the new LOX/RNO method. Adv. Hort. Sci., 29, 9.

[3] Young, A. J., & Lowe, G. L. (2018). Carotenoids-Antioxidant Properties. Antioxidants (Basel), 7 (2).

[4] Rodriguez-Maturino, A., Troncoso-Rojas, R., Sanchez-Estrada, A., Gonzalez-Mendoza, D., Ruiz-Sanchez, E., Zamora-Bustillos, R., Cecena-Duran, C., Grimaldo-Juarez, O., & Aviles-Marin, M. (2015). [Antifungal effect of phenolic and carotenoids extracts from chiltepin (Capsicum annum var. glabriusculum) on Alternaria alternata and Fusarium oxysporum]. Rev Argent Microbiol, 47 (1), 72-77.

[5] Lee, W., & Lee, D. G. (2014). Lycopene-induced hydroxyl radical causes oxidative DNA damage in Escherichia coli. J Microbiol Biotechnol, 24 (9), 1232-1237.

[6] Songca, S. P., Sebothoma, C., Samuel, B. B., & Eloff, J. N. (2012). A Biflavonoid and a Carotenoid from Rhus leptodictya: Isolation, Characterization and Antibacterial Properties. African Journal of Biochemistry Research, 6, 7.

[7] Hernandez-Ortega, M., Ortiz-Moreno, A., Hernandez-Navarro, M. D., Chamorro-Cevallos, G., Dorantes-Alvarez, L., & Necoechea-Mondragon, H. (2012). Antioxidant, antinociceptive, and anti-inflammatory effects of carotenoids extracted from dried pepper (Capsicum annuum L.). J Biomed Biotechnol, 2012, 524019.

[8] Festuccia, C., Mancini, A., Gravina, G. L., Scarsella, M., Llorens, S., Alonso, G. L., Tatone, C., Di Cesare, E., Jannini, E. A., Lenzi, A., D'Alessandro, A. M., & Carmona, M. (2014). Antitumor effects of saffron-derived carotenoids in prostate cancer cell models. Biomed Res Int, 2014, 135048.

[9] Linnewiel-Hermoni, K., Khanin, M., Danilenko, M., Zango, G., Amosi, Y., Levy, J., & Sharoni, Y. (2015). The anti-cancer effects of carotenoids and other phytonutrients resides in their combined activity. Arch Biochem Biophys, 572, 28-35.

[10] Meléndez-Martínez, A. J., Mandić, A. I., Bantis, F., Böhm, V., Borge, G. I. A., Brnčić, M., Bysted, A., Cano, M. P., Dias, G., Elgersma, A., Fikselová, M., García-Alonso, J., Giuffrida, D., Gonçalves, V. N. N., Hornero-Méndez, D., Kljak, K., Lavelli, V., Manganaris, G.A., Mapelli-Brahm, P., Marounek, M., Olmedilla-Alonso, B., Periago-Castón, M.J., Pintea, A., Sheehan, J.J., Šaponjac, V.T., Valšíková-Frey, M., Meulebroek, L. & O'Brien, N. (2020). A comprehensive review on carotenoids in foods and feeds: Status quo, applications, patents, and research needs. Critical reviews in food science and nutrition, 1-51.

[11] Ascenso, A., Pedrosa, T., Pinho, S., Pinho, F., de Oliveira, J. M., Cabral Marques, H., Oliveira, H., Simoes, S., & Santos, C. (2016). The Effect of Lycopene Preexposure on UV-B-Irradiated Human Keratinocytes. Oxid Med Cell Longev, 2016, 8214631.

[12] Edge, R., & Truscott, T. G. (2018). Singlet Oxygen and Free Radical Reactions of Retinoids and Carotenoids-A Review. Antioxidants (Basel), 7 (1).

[13] Kawata, A., Murakami, Y., Suzuki, S., & Fujisawa, S. (2018). Anti-inflammatory Activity of beta-Carotene, Lycopene and Tri-n-butylborane, a Scavenger of Reactive Oxygen Species. In Vivo, 32 (2), 255-264.

[14] Vasconcelos, A. G., Amorim, A., Dos Santos, R. C., Souza, J. M. T., de Souza, L. K. M., Araujo, T. S. L., Nicolau, L. A. D., de Lima Carvalho, L., de Aquino, P. E. A., da

Silva Martins, C., Ropke, C. D., Soares, P. M. G., Kuckelhaus, S. A. S., Medeiros, J. R., & Leite, J. (2017). Lycopene rich extract from red guava (Psidium guajava L.) displays anti-inflammatory and antioxidant profile by reducing suggestive hallmarks of acute inflammatory response in mice. Food Res Int, 99 (Pt 2), 959-968.

[15] Choi, H., & Lee, D. G. (2015). Lycopene induces apoptosis in Candida albicans through reactive oxygen species production and mitochondrial dysfunction. Biochimie, 115, 108-115.

[16] Desai, P. R., Holihosur, P. D., Marathe, S. V., Kulkarni, B. B., Vishal, U. K., K., G. R., Rajeev, R. P., & V., H. S. (2018). Studies on Isolation and Quantification of Lycopene from Tomato and Papaya and its Antioxidant and Antifungal Properties. International Journal of Agriculture Innovations and Research, 6, 4.

[17] Muller, L., Caris-Veyrat, C., Lowe, G., & Bohm, V. (2016). Lycopene and Its Antioxidant Role in the Prevention of Cardiovascular Diseases-A Critical Review. Crit Rev Food Sci Nutr, 56 (11), 1868-1879.

[18] Xu, J., Hu, H., Chen, B., Yue, R., Zhou, [illegible] Liu, Y., Zhang, S., Xu, L., Wang, H., & Yu, Z. (2015). Lycopene Protects against Hypoxia/Reoxygenation Injury by Alleviating ER Stress Induced Apoptosis in Neonatal Mouse Cardiomyocytes. PLoS One, 10 (8), e0136443.

[19] Bhardwaj, M., & Kumar, A. (2016). Neuroprotective Effect of Lycopene Against PTZ-induced Kindling Seizures in Mice: Possible Behavioural, Biochemical and Mitochondrial Dysfunction. Phytother Res, 30 (2), 306-313.

[20] Prema, A., Janakiraman, U., Manivasagam, T., & Thenmozhi, A. J. (2015). Neuroprotective effect of lycopene against MPTP induced experimental Parkinson's disease in mice. Neurosci Lett, 599, 12-19.

[21] Tan, H. L., Thomas-Ahner, J. M., Moran, N. E., Cooperstone, J. L., Erdman, J. W., Jr., Young, G. S., & Clinton, S. K. (2017). beta-Carotene 9',10' Oxygenase Modulates the Anticancer Activity of Dietary Tomato or Lycopene on Prostate Carcinogenesis in the TRAMP Model. Cancer Prev Res (Phila), 10 (2), 161-169.

[22] Holzapfel, N. P., Shokoohmand, A., Wagner, F., Landgraf, M., Champ, S., Holzapfel, B. M., Clements, J. A., Hutmacher, D. W., & Loessner, D. (2017). Lycopene reduces ovarian tumor growth and intraperitoneal metastatic load. Am J Cancer Res, 7 (6), 1322-1336.

[23] Arathi, B. P., Raghavendra-Rao Sowmya, P., Kuriakose, G. C., Shilpa, S., Shwetha, H. J., Kumar, S., Raju, M., Baskaran, V., & Lakshminarayana, R. (2018). Fractionation

and Characterization of Lycopene-Oxidation Products by LC-MS/MS (ESI)(+): Elucidation of the Chemopreventative Potency of Oxidized Lycopene in Breast-Cancer Cell Lines. J Agric Food Chem, 66 (43), 11362-11371.

[24] Peng, S. J., Li, J., Zhou, Y., Tuo, M., Qin, X. X., Yu, Q., Cheng, H., & Li, Y. M. (2017). In vitro effects and mechanisms of lycopene in MCF-7 human breast cancer cells. Genet Mol Res, 16 (2).

[25] Ganesh, N. S. K., Lakshmi, B., & Chandy, V. (2016). Lycopene properties and it's benefits in human health: Brief Review. World Journal of Pharmacy and Pharmaceutical Sciences, 5 (12), 13.

[26] Tan, B. L., & Norhaizan, M. E. (2019). Carotenoids: How Effectiv Age-Related Diseases? Molecules, 24, 23.

[27] Pelissari, J. R., Souza, V. B., Pigoso, A. A., Tubini, F. L., Thomazini, M., Rodrigues, C. E. C., Urbano, A., & Favaro-Trindade, C. S. (2015). Production of solid lipid microparticles loaded with lycopene by spray chilling: Structural characteristics of particles and lycopene stability. Food and Bioproducts Processing, 98, 9.

[28] Meléndez-Martínez, A. J., Böhm, V., Borge, G. I. A., Cano, M. P., Fikselová, M., Gruskiene, R., Lavelli, V., Loizzo, M. R., Mandi´c, A.I., Brahm, P.M., Mišan, A.C., Pintea, A.M., Sereikaitˇe, J., Vargas-Murga, J., Vlaisavljevi´c, S.S., Vuli´c, J.J. & O'Brien, N. M. (2021). Carotenoids: Considerations for Their Use in Functional Foods, Nutraceuticals, Nutricosmetics, Supplements, Botanicals, and Novel Foods in the Context of Sustainability, Circular Economy, and Climate Change. Annual Review of Food Science and Technology, 12, 433-460.

[29] Nazemiyeh, E., Eskandani, M., Sheikhloie, H., & Nazemiyeh, H. (2016). Formulation and Physicochemical Characterization of Lycopene-Loaded Solid Lipid Nanoparticles. Adv Pharm Bull, 6 (2), 235-241.

[30] Okonogi, S., & Riangjanapatee, P. (2015). Physicochemical characterization of lycopene-loaded nanostructured lipid carrier formulations for topical administration. Int J Pharm, 478 (2), 726-735.

[29] Shi, J., Xue, S. J., Wang, B., Wang, W., Ye, X., & Quek, S. Y. (2015). Optimization of formulation and influence of environmental stresses on stability of lycopene-microemulsion. LWT - Food Science and Technology 60, 10.

[30] Rao, J. P., & Geckeler, K. E. (2011). Polymer nanoparticles: Preparation techniques and size-control parameters. Progress in Polymer Science, 36, 27.

[31] Martinez-Ballesta, M., Gil-Izquierdo, A., Garcia-Viguera, C., & Dominguez-Perles, R. (2018). Nanoparticles and Controlled Delivery for Bioactive Compounds: Outlining Challenges for New "Smart-Foods" for Health. Foods, 7 (5).

[32] Zorzi, G. K., Carvalho, E. L. S., Lino von Poser, G., & Teixeira, H. F. (2015). On the use of nanotechnology-based strategies for association of complex matrices from plant extracts. Revista Brasileira de Farmacognosia, 25, 11.

[33] Han, J., Zhao, D., Li, D., Wang, X., Jin, Z., & Zhao, K. (2018). Polymer-Based Nanomaterials and Applications for Vaccines and Drugs. Polymers (Basel), 10 (1).

[34] Rangari, A., & Ravikumar, P. (2015.). Polymeric Nanoparticles Based Topical Drug Delivery: An Overview. Asian Journal of Biomedical and Pharmaceutical Sciences, 5, 8.

[35] Yadav, H. K. S., Almokdad, A. A., Shaluf, S. I. M., & Debe, M. S. (2019). Polymer-BasedNanomaterials forDrug-Delivery Carriers Nanocarriers for Drug Delivery.

[36] Amorim, A. G. N., Pintado, M. E., & Leite, J. R. S. (2018). Obtetion process of carotenoids concentrate rich in lycopene from red fruits and/or red fruit pulp. patent nº EP20180171653 20180509.

[38] Santos, R. C., Ombredane, A. S., Souza, J. M. T., Vasconcelos, A. G., Placido, A., Amorim, A., Barbosa, E. A., Lima, F., Ropke, C. D., Alves, M. M. M., Arcanjo, D. D. R., Carvalho, F. A. A., Delerue-Matos, C., Joanitti, G. A., & Leite, J. (2018). Lycopene-rich extract from red guava (Psidium guajava L.) displays cytotoxic effect against human breast adenocarcinoma cell line MCF-7 via an apoptotic-like pathway. Food Res Int, 103, 184-196.

[39] Amorim, A. G. N., Souza, J. M. T., Santos, R. C., Gullon, B., Oliveira, A., Santos, L. F. A., Virgino, A. L. E., Mafud, A. C., Petrilli, H. M., Mascarenhas, Y. P., Delerue-Matos, C., Pintado, M. E., & Leite, J. R. S. A. (2018). HPLC-DAD, ESI–MS/MS, and NMR of Lycopene Isolated From P. guajava L. and Its Biotechnological Applications. Eur. J. Lipid Sci. Technol., 13.

[40] De Paula, R. C. M., Heatley, F., & Budd, P. M. (1998). Characterization of Anacardiumoccidentale exudate polysaccharide. Polymer International, 45, 15.

[41] Araújo, I. M. S., Zampa, M. F., Moura, J. B., dos Santos Jr, J. R., Eaton, P., Zucolotto, V., Veras, L. M. C., De Paula, R. C. M., Feitosa, J. P. A., Leite, J. R. S. A., & Eiras, C. (2012). Contribution of the cashew gum (Anacardium occidentale L.) for development of layer-by-layer films with potential application in nanobiomedical devices. Materials Science and Engineering C, 32, 6.

[42] Pitombeira, N. A., Veras Neto, J. G., Silva, D. A., Feitosa, J. P., Paula, H. C., & de Paula, R. C. (2015). Self-assembled nanoparticles of acetylated cashew gum: characterization and evaluation as potential drug carrier. Carbohydr Polym, 117, 610-615.

[43] Wang, C. Y., & Chen, Y. C. (2015). Extraction and Characterization of fucoidan from six brown macroalgae. Journal of Marine Science and Technology, 19.

[44] Gharib, A., & Faezizadeh, Z. (2014). In vitro anti-telomerase activity of novel lycopene-loaded nanospheres in the human leukemia cell line K562. Pharmacogn Mag, 10 (Suppl 1), S157-163.

[45] Li, W., Yalcin, M., Lin, Q., Ardawi, M. M., & Mousa, S. A. (2017). Self-assembly of green tea catechin derivatives in nanoparticles for oral lycopene delivery. J Control Release, 248, 117-124.

[46] Mendes, M., Carvalho, A. P., Magalhães, J. M. C. S., Moreira, M., Guido, L., Gomes, A. M., & Delerue-Matos, C. (2016). Response surface evaluation of microwave-assisted extraction conditions for Lycium barbarum bioactive compounds. Innovative Food Science and Emerging Technologies, 33, 8.

[47] Vasconcelos, A. G., Valima, M. O., Amorim, A. G. N., Amaral, C. P., Almeida, M. P., Borges, T. K. S., Socodato, R., Portugal, C. C., Brand, G. D., Mattos, J. S. C., Relvas, J. B., Plácido, A., Eaton, P., Ramos, D. A. R., Kückelhaus, S. A. S., & Leite, J. R. S. A. (2020). Cytotoxic activity of poly-ε-caprolactone lipid-core nanocapsules loaded with lycopene-rich extract from red guava (Psidium guajava L.) on breast cancer cells. Food Res Int, 136, 12.

[48] Ignasiak, K., & Maxwell, A. (2017). Galleria mellonella (greater wax moth) larvae as a model for antibiotic susceptibility testing and acute toxicity trials. BMC Res Notes, 10 (1), 428.

[49] Nascimento Dias, J., de Souza Silva, C., de Araujo, A. R., Souza, J. M. T., de Holanda Veloso Junior, P. H., Cabral, W. F., da Gloria da Silva, M., Eaton, P., de Souza de Almeida Leite, J. R., Nicola, A. M., Albuquerque, P., & Silva-Pereira, I. (2020). Mechanisms of action of antimicrobial peptides ToAP2 and NDBP-5.7 against Candida albicans planktonic and biofilm cells. Sci Rep, 10 (1), 10327.

[50] Gupta, P., Bansal, M. P., & Koul, A. (2013). Spectroscopic characterization of lycopene extract from Lycopersicum esculentum (Tomato) and its evaluation as a chemopreventive agent against experimental hepatocarcinogenesis in mice. Phytother Res, 27 (3), 448-456.

[51] Bunghez, I. R., Raduly, M., Doncea, S., Aksahin, I., & Ion, R. M. (2011). Lycopene determination in tomatoes by different spectral techniques (uv-vis, ftir and hplc). Digest Journal of Nanomaterials and Biostructures, 6 (3), 8.

[52] Holzapfel, N. P., Holzapfel, B. M., Champ, S., Feldthusen, J., Clements, J., & Hutmacher, D. W. (2013). The potential role of lycopene for the prevention and therapy of prostate cancer: from molecular mechanisms to clinical evidence. Int J Mol Sci, 14 (7), 14620-14646.

[53] Swierczewska, M., Han, H. S., Kim, K., Park, J. H., & Lee, S. (2016). Polysaccharide-based nanoparticles for theranostic nanomedicine. Adv Drug Deliv Rev, 99 (Pt A), 70-84.

[54] Sharma, N., Madan, P., & Lin, S. (2016). Effect of process and formulation variables on the preparation of parenteral paclitaxel-loaded biodegradable polymeric nanoparticles: A co-surfactant study. Asian Journal of Pharmaceutical Sciences, 13.

[55] Kheradmandnia, S., Vasheghani-Farahani, E., Nosrati, M., & Atyabi, F. (2010). Preparation and characterization of ketoprofen-loaded solid lipid nanoparticles made from beeswax and carnauba wax. Nanomedicine, 6 (6), 753-759.

[56] Rodrigues, J. A., Araujo, A. R., Pitombeira, N. A., Placido, A., de Almeida, M. P., Veras, L. M. C., Delerue-Matos, C., Lima, F., Neto, A. B., de Paula, R. C. M., Feitosa, J. P. A., Eaton, P., Leite, J., & da Silva, D. A. (2019). Acetylated cashew gum-based nanoparticles for the incorporation of alkaloid epiisopiloturine. Int J Biol Macromol, 128, 965-972.

[57] Mora-Huertas, C. E., Fessi, H., & Elaissari, A. (2010). Polymer-based nanocapsules for drug delivery. Int J Pharm, 385 (1-2), 113-142.

[58] Banerjee, A., Qi, J., Gogoi, R., Wong, J., & Mitragotri, S. (2016). Role of nanoparticle size, shape and surface chemistry in oral drug delivery. J Control Release, 238, 176-185.

[59] Danaei, M., Dehghankhold, M., Ataei, S., Hasanzadeh Davarani, F., Javanmard, R., Dokhani, A., Khorasani, S., & Mozafari, M. R. (2018). Impact of Particle Size and Polydispersity Index on the Clinical Applications of Lipidic Nanocarrier Systems. Pharmaceutics, 10 (2).

[60] Johnston, S. T., Faria, M., & Crampin, E. J. (2018). An analytical approach for quantifying the influence of nanoparticle polydispersity on cellular delivered dose. J R Soc Interface, 15 (144).

[61] Akhoond Zardini, A., Mohebbi, M., Farhoosh, R., & Bolurian, S. (2018). Production and characterization of nanostructured lipid carriers and solid lipid nanoparticles containing lycopene for food fortification. J Food Sci Technol, 55 (1), 287-298.

[62] Park, S. J., Garcia, C. V., Shin, G. H., & Kim, J. T. (2017). Development of nanostructured lipid carriers for the encapsulation and controlled release of vitamin D3. Food Chem, 225, 213-219.

[63] Witayaudom, P., & Klinkesorn, U. (2017). Effect of surfactant concentration and solidification temperature on the characteristics and stability of nanostructured lipid carrier (NLC) prepared from rambutan (Nephelium lappaceum L.) kernel fat. J Colloid Interface Sci, 505, 1082-1092.

[64] Crucho, C. I. C., & Barros, M. T. (2017). Polymeric nanoparticles: A study on the preparation variables and characterization methods. Mater Sci Eng C Mater Biol Appl, 80, 771-784.[65] Filipe, V., Hawe, A., & Jiskoot, W. (2010). Critical evaluation of Nanoparticle Tracking Analysis (NTA) by NanoSight for the measurement of nanoparticles and protein aggregates. Pharm Res, 27 (5), 796-810.

[66] Tang, S. Y., et al. (2019). Phase separation in liquid metal nanoparticles. Matter, v. 1, n. 1, p. 192-204.

[67] Demiray, E., Tulek, Y., & Yilmaz, Y. (2013). Degradation kinetics of lycopene, β-carotene and ascorbic acid in tomatoes during hot air drying. LWT-Food Science and Technology, 50(1), 172-176.

[68] Manzo, N., Santini, A., Pizzolongo, F., Aiello, A., & Romano, R. (2019). Degradation kinetic (D100) of lycopene during the thermal treatment of concentrated tomato paste. **Natural product research**, 33(13), 1835-1841.

[69] Kestens, V., Bozatzidis, V., Temmerman, P. J., Ramaye, Y., & Roebben, G. (2017). Validation of a particle tracking analysis method for the size determination of nano- and microparticles. J Nanopart Res, 19 (8), 271.

[70] Eaton, P., Quaresma, P., Soares, C., Neves, C., de Almeida, M. P., Pereira, E., & West, P. (2017). A direct comparison of experimental methods to measure dimensions of synthetic nanoparticles. Ultramicroscopy, 182, 179-190.

[71] Ruozi, B., Belletti, D., Vandelli, M. A., Pederzoli, F., Veratti, P., Forni, F., Tosi, G., Tonelli, M., & Zapparoli, M. (2014). AFM/TEM Complementary Structural Analysis of Surface-Functionalized Nanoparticles. J Phys Chem Biophys, 4, 7.

[72] Pereira, M. C., Hill, L. E., Zambiazi, R. C., Mertens-Talcott, S., Talcott, S., & Gomes, C. L. (2015). Nanoencapsulation of hydrophobic phytochemicals using poly (DL-lactide-co-glycolide) (PLGA) for antioxidant and antimicrobial delivery applications:

Guabiroba fruit (Campomanesia xanthocarpa O. Berg) study. LWT - Food Science and Technology, 63, 8.

[73] Tsapis, N. (2016). Imaging Polymer Nanoparticles by Means of Transmission and Scanning Electron Microscopy Techniques. Polymer Nanoparticles for Nanomedicines, 15.

[74] Gupta, P., Authimoolam, S. P., Hilt, J. Z., & Dziubla, T. D. (2015). Quercetin conjugated poly(beta-amino esters) nanogels for the treatment of cellular oxidative stress. Acta Biomater, 27, 194-204.

[75] Souza, T. G. F., Ciminelli, V. S. T., & Mohallem, N. D. S. (2015). An assessment of errors in sample preparation and data processing for nanoparticle size analyses by AFM. Materials Characterization, 109, 8.

[76] Oliveira, A. C. J., Araujo, A. R., Quelemes, P. V., Nadvorny, D., Soares-Sobrinho, J. L., Leite, J., da Silva-Filho, E. C., & Silva, D. A. D. (2019). Solvent-free production of phthalated cashew gum for green synthesis of antimicrobial silver nanoparticles. Carbohydr Polym, 213, 176-183.

[77] Dias, S. F., Nogueira, S. S., de França Dourado, F., Guimaraes, M. A., de Oliveira Pitombeira, N. A., Gobbo, G. G., Primo, F. L., de Paula, R. C., Feitosa, J. P., Tedesco, A. C., Nunes, L. C., Leite, I. F., & da Silva, D. A. (2016). Acetylated cashew gum-based nanoparticles for transdermal delivery of diclofenac diethyl amine. Carbohydr Polym, 143, 254-261.

[78] Silva, E., L, V , Patriota, Y. B. G., Ribeiro, A. J., Veiga, F., Hallwass, F., Silva-Filho, E. C., da Silva, D. A., Soares, M. F. R., Wanderley, A. G., & Soares-Sobrinho, J. L. (2019). Solvent-free synthesis of acetylated cashew gum for oral delivery system of insulin. Carbohydr Polym, 207, 601-608.

[79] Dantas-Santos, N., Almeida-Lima, J., Vidal, A. A. J., Gomes, D. L., Oliveira, R. M., Pedrosa, S. S., Pereira, P., Gama, F. M., & Rocha, H. A. O. (2012). Antiproliferative Activity of Fucan Nanogel. Mar. Drugs, 10, 22.

[80] Fernandes-Negreiros, M. M., Araujo Machado, R. I., Bezerra, F. L., Nunes Melo, M. C., Alves, M., Alves Filgueira, L. G., Morgano, M. A., Trindade, E. S., Costa, L. S., & Rocha, H. A. O. (2017). Antibacterial, Antiproliferative, and Immunomodulatory Activity of Silver Nanoparticles Synthesized with Fucans from the Alga Dictyota mertensii. Nanomaterials (Basel), 8 (1).

[81] Vasantharaja, R., Stanley Abraham, L., Gopinath, V., Hariharan, D., & Smita, K. M. (2019). Attenuation of oxidative stress induced mitochondrial dysfunction and

cytotoxicity in fibroblast cells by sulfated polysaccharide from Padina gymnospora. Int J Biol Macromol, 124, 50-59.

[82] Priam, F., Marcelin, O., Marcus, R., Jô, L. F., & Smith-Ravin, E. J. (2017). Lycopene extraction from Psidium guajava L. and evaluation of its antioxidant properties using a modified DPPH test. Journal of Environmental Science, Toxicology and Food Technology, 11, 7.

[83] Nascimento, T. G., da Silva, P. F., Azevedo, L. F., da Rocha, L. G., de Moraes Porto, I. C., Lima, E. M. T. F., Basilio-Junior, I. D., Grillo, L. A., Dornelas, C. B., Fonseca, E. J., de Jesus Oliveira, E., Zhang, A. T., & Watson, D. G. (2016). Polymeric Nanoparticles of Brazilian Red Propolis Extract: Preparation, Characterization, Antioxidant and Leishmanicidal Activity. Nanoscale Res Lett, 11 (1), 301.

[84] Barbosa, E. A., Oliveira, A., Placido, A., Socodato, R., Portugal, C. C., Mafud, A. C., Ombredane, A. S., Moreira, D. C., Vale, N., Bessa, L. J., Joanitti, G. A., Alves, C., Gomes, P., Delerue-Matos, C., Mascarenhas, Y. P., Marani, M. M., Relvas, J. B., Pintado, M., & Leite, J. (2018). Structure and function of a novel antioxidant peptide from the skin of tropical frogs. Free Radic Biol Med, 115, 68-79.

[85] Amorim, A., Souza, J., Oliveira, A., Santos, R., Vasconcelos, A., Souza, L., Araujo, T., Cabral, W., Silva, M., Mafud, A., Mascarenhas, Y., Medeiros, J. V., Saraiva, J., Muehlmann, L., Kuckelhaus, S., Pintado, M., & Leite, J. R. (2020). Anti-inflammatory and antioxidant activity improvement of lycopene from guava on nanoemulsifying system. Journal of Dispersion Science and Technology, 12.

[86] Pereira, M. C., Oliveira, D. A., Hill, L. E., Zambiazi, R. C., Borges, C. D., Vizzotto, M., Mertens-Talcott, S., Talcott, S., & Gomes, C. L. (2018). Effect of nanoencapsulation using PLGA on antioxidant and antimicrobial activities of guabiroba fruit phenolic extract. Food Chem, 240, 396-404.

[87] Donahue, N. D., Acar, H., & Wilhelm, S. (2019). Concepts of nanoparticle cellular uptake, intracellular trafficking, and kinetics in nanomedicine. Adv Drug Deliv Rev, 143, 68-96.

[88] Puri, R., Adesina, S., & Akala, E. (2018). Cellular uptake and cytotoxicity studies of pH-responsive polymeric nanoparticles fabricated by dispersion polymerization. J Nanosci Nanomed., 2, 16.

[89] Akl, M. A., Kartal-Hodzic, A., Oksanen, T., Ismael, H. R., Afouna, M. M., Yliperttula, M., Samy, A. M., & Viitala, T. (2016). Factorial design formulation optimization and

in vitro characterization of 2 curcumin-loaded PLGA nanoparticles for colon delivery. Journal of Drug Delivery Science and Technology, 32, 10.

[90] Bao, H., Zhang, Q., Xu, H., & Yan, Z. (2016). Effects of nanoparticle size on antitumor activity of 10-hydroxycamptothecin-conjugated gold nanoparticles: in vitro and in vivo studies. Int J Nanomedicine, 11, 929-940.

[91] Yang, Y., Pan, D., Luo, K., Li, L., & Gu, Z. (2013). Biodegradable and amphiphilic block copolymer-doxorubicin conjugate as polymeric nanoscale drug delivery vehicle for breast cancer therapy. Biomaterials, 34 (33), 8430-8443.

[92] Dobrovolskaia, M. A., Clogston, J. D., Neun, B. W., Hall, J. B., Patri, A. K., & McNeil, S. E. (2008). Method for analysis of nanoparticle hemolytic properties in vitro. Nano Lett, 8 (8), 2180-2187.

[93] Pan, D., Vargas-Morales, O., Zern, B., Anselmo, A. C., Gupta, V., Zakrewsky, M., Mitragotri, S., & Muzykantov, V. (2016). The Effect of Polymeric Nanoparticles on Biocompatibility of Carrier Red Blood Cells. PLoS One, 11 (3), e0152074.

[94] Chiste, R. C., Freitas, M., Mercadante, A. Z., & Fernandes, E. (2014). Carotenoids inhibit lipid peroxidation and hemoglobin oxidation, but not the depletion of glutathione induced by ROS in human erythrocytes. Life Sci, 99 (1-2), 52-60.

[95] Desbois, A. P., & Coote, P. J. (2012). Utility of Greater Wax Moth Larva (Galleria mellonella) for Evaluating the Toxicity and Efficacy of New Antimicrobial Agents. Adv Appl Microbiol, 78, 25-53.[

[96] Spadari, C. C., de Bastiani, F., Lopes, L. B., & Ishida, K. (2019). Alginate nanoparticles as non-toxic delivery system for miltefosine in the treatment of candidiasis and cryptococcosis. Int J Nanomedicine, 14, 5187-5199.

Table 1. Composition and characterization of nanoparticles: particle size, zeta potential, polydispersity index (PDI) and incorporation efficiency (IE).

NPs	OP		AP	Coating	Size (nm)*	PDI*	ZP (mV)	EE (%)
	LEG (mg)	CGa (mg)	T80 (mg)	FUC (mg)				
NBGa	-	10	7	-	189.3±0.4	0.25±0.02	-26.5±1.1	-
NGa1	10	10	7	-	215.5±0.5	0.20±0.00	-23.3±0.3	13.0±0.2
NGa2	10	10	14	-	251.1±3.5	0.20±0.01	-17.5±1.2	8.5±0.4
NBFGa	-	10	33	10	272.0±11.3	0.46±0.01	-29.9±0.9	-
NFGa	10	10	33	10	162.0±3.3	0.35±0.02	-30.7±1.3	60.0±0.1

* Data obtained by Dynamic Light Sacattering (DLS). The data were expressed as mean ± standard deviation. NPs: nanoparticles; OP: organic phase; AP: aqueous phase; LEG:

lycopene-rich extract from red guava; CGa: acetylated cashew gum; T80: tween 80; FUC: fucan. PDI: polydispersity index; ZP: zeta potential; EE: encapsulation efficiency.

Table 2. Size, polydispersity index (PDI), zeta potential (ZP) and pH of the nanoparticles over 30, 60 and 90 days at 4ºC and 27ºC.

Temperature	Sample	Period	Size (nm)*	PDI*	ZP (mV)	pH
4 °C	NGa1	30 days	215.5	0.197	-23.3	4.3
		60 days	-	-	-	-
		90 days	-	-	-	-
			215.5	**0.197**	**-23.3**	**4.3**
	NGa2	30 days	251.1	0.202	17.5	5.1
		60 days	-	-	-	-
		90 days	-	-	-	-
			251.1	**0.202**	**-17.5**	**5.1**
	NFGa	30 days	160.9	0.336	-29.5	6.7
		60 days	159.5	0.338	-30.5	6.6
		90 day	165.7	0.371	-32.1	6.7
			162.0	**0.348**	**-30.7**	**6.7**
27 °C	NFGa	30 days	258.9	0.539	-23.2	5.7
		60 days	-	-	-	-
		90 days	-	-	-	-
			258.9	**0.539**	**-23.2**	**5.7**

* Data obtained by Dynamic Light Scattering (DLS). - Periods without information on the parameters due to the degradation of the sample.

Table 3. Quantitative data of the antioxidant activity of NFGa.

Antioxidant assay	TEAC (µM Trolox/mL de nanoparticles)
ABTS	93.7 ± 1.1
ORAC	2267.0 ± 70.8

Legend of figures

Fig. 1. UV-Vis spectrum (A) and chromatogram (B) of the lycopene standard (LS) and lycopene-rich extract from red guava (LEG).

Fig. 2. Representation of acetylation of cashew gum.

Fig. 3. Characterization by UV-VIS spectrophotometry of the blank nanoparticles with (D) and without (A) fucan coating and nanoparticles containing LEG with (E) and without (B and C) fucan coating.

Fig. 4. Analysis of the size distribution and concentration of NFGa by NTA technique.

Fig. 5: Morphological characteristics of nanoparticles. In A and B, image by TEM of NBFGa and NFGa respectively. Images by AFM in 3D and 2D respectively of NBFGa in C and D and NFGa in E and F.

Fig. 6. Fourier Transform Infrared Spectroscopy (FTIR) characterization of cashew gum (CG), acetylated cashew gum (CGa), fucan (FUC), lycopenerich extract from red guava (LEG), fucan-coated acetylated cashew gum nanparticles containing LEG (NFGa) and fucan-coated acetylated cashew gum nanparticles without LEG (NBFGa).

Fig. 7. Effect of lycopene-rich extract from red guava (LEG) (A), NBFGa (B) and NFGa (C) on cell viability in MCF-7 cell line for a period of 24 and 72 hours. Values were expressed as means ± SEM. ** p<0.01 versus 24 h DMEM control group. **** p <0.0001 versus 24 h DMEM control group. # p<0.0001 versus 72 h DMEM control group.

Fig. 8. Effect of lycopene-rich extract from red guava (LEG) (A), NBFGa (B) and NFGa (C) on cell viability in HaCaT cell line for a period of 24 and 72 hours. Values were expressed as means ± SEM. * *p*<0.05 versus 24 h DMEM control group. *** *p* <0.001 versus 24 h DMEM control group. # *p*<0.0001 versus 72 h DMEM control group.

Fig. 9. Hemolytic activity of NFGa and NBFGa in sheep erythrocytes (A) and survival curve of *G. mellonella* larvae after inoculation of different doses of NFGa (5, 10 and 20 mg kg) (B).

Fig.1

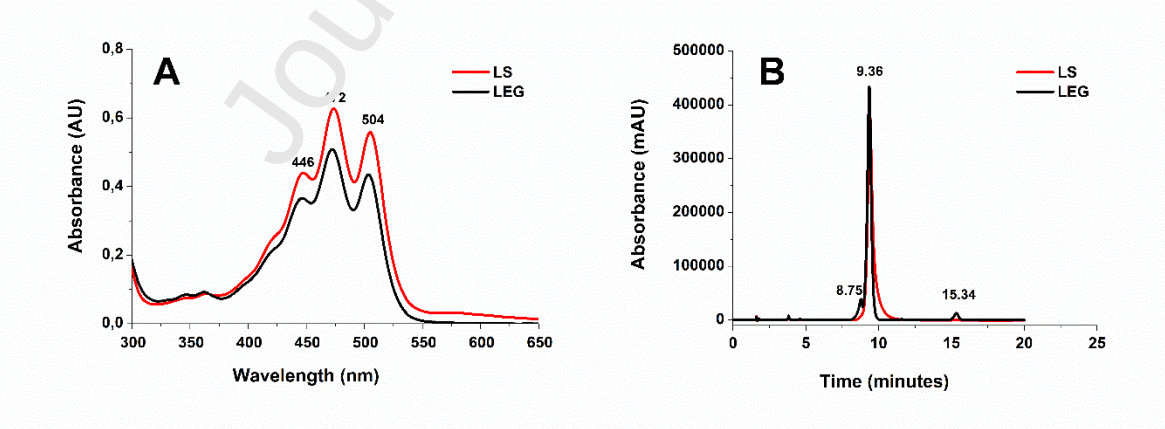

Fig. 2

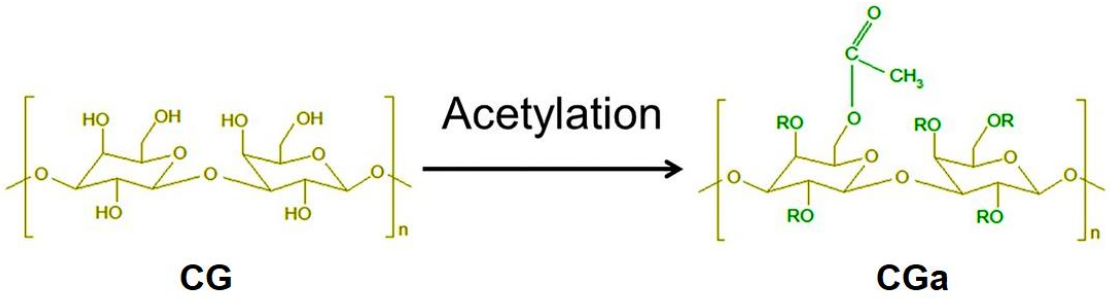

Fig. 3

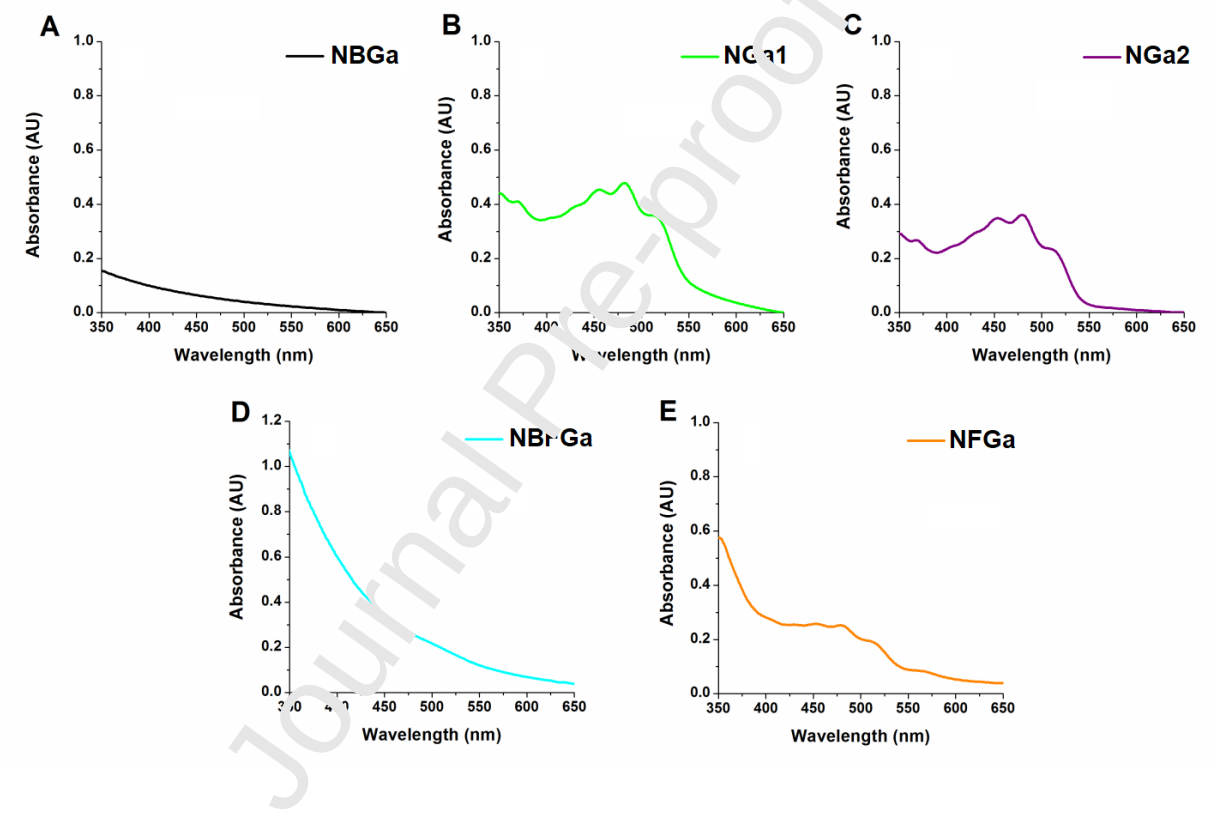

Fig. 4

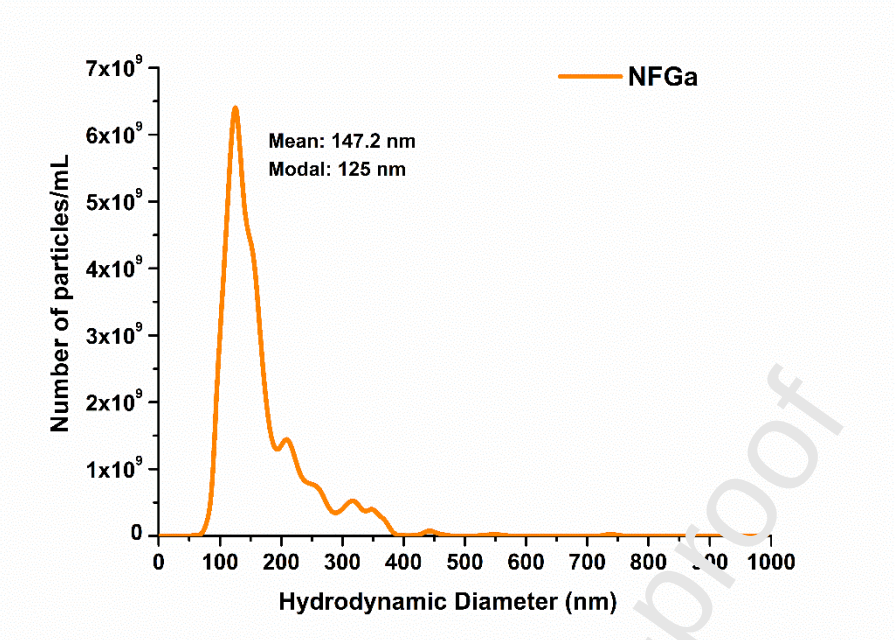

Fig. 5

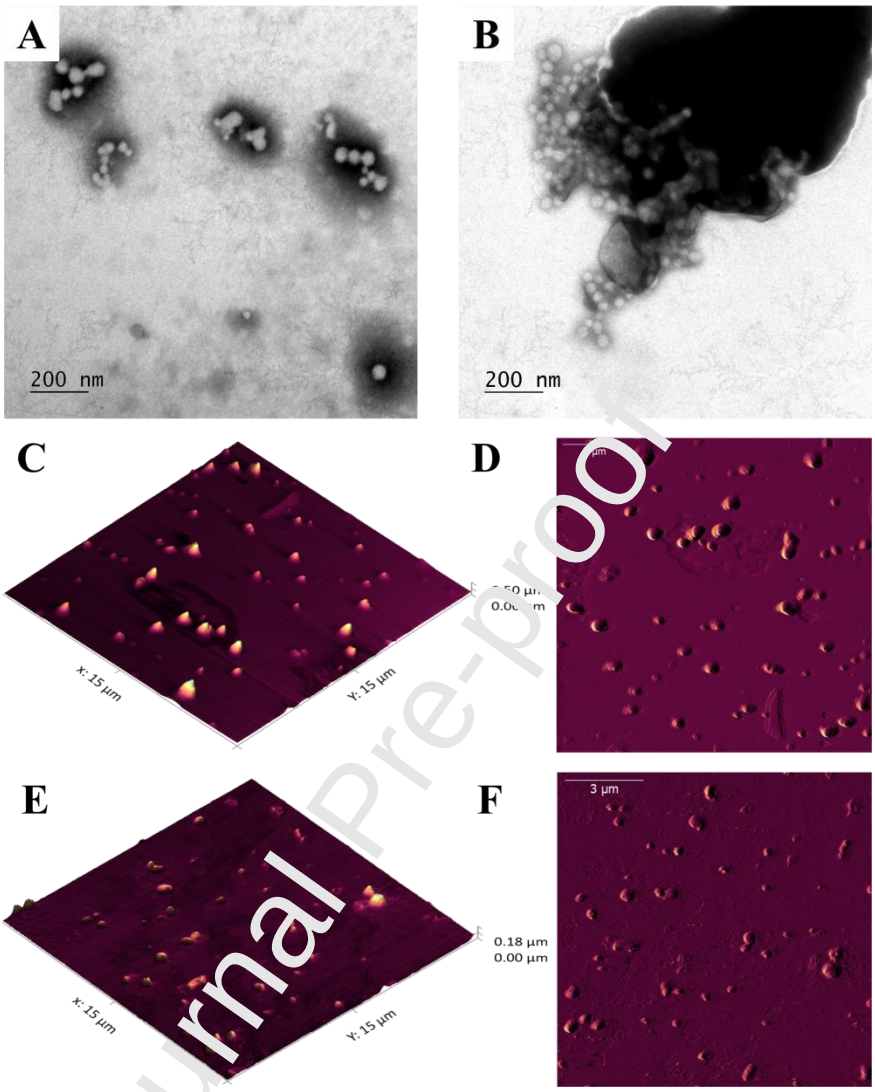

Fig. 6

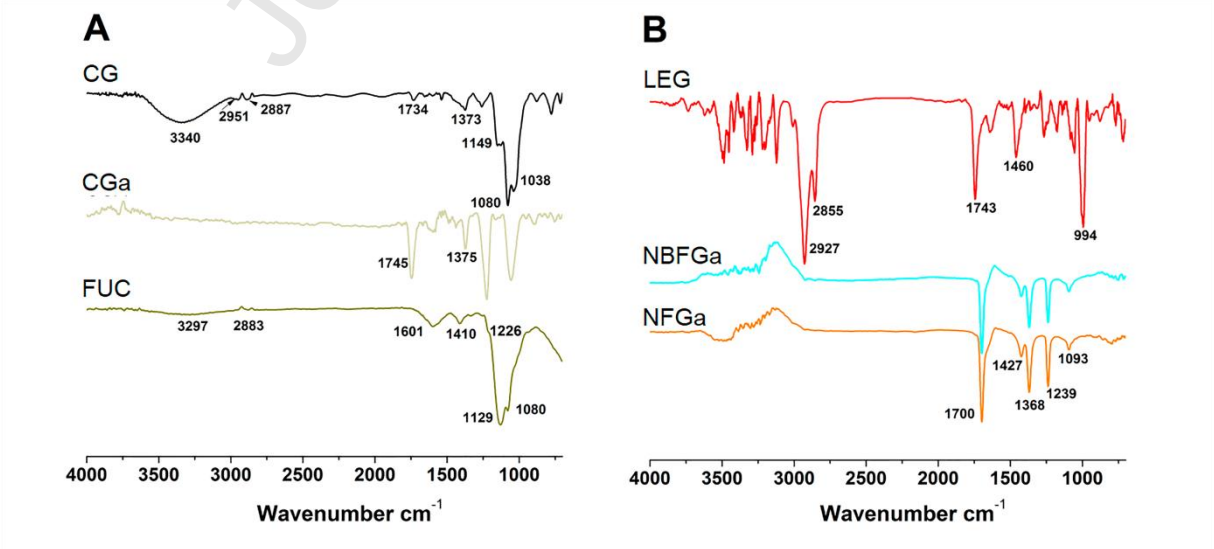

Fig. 7

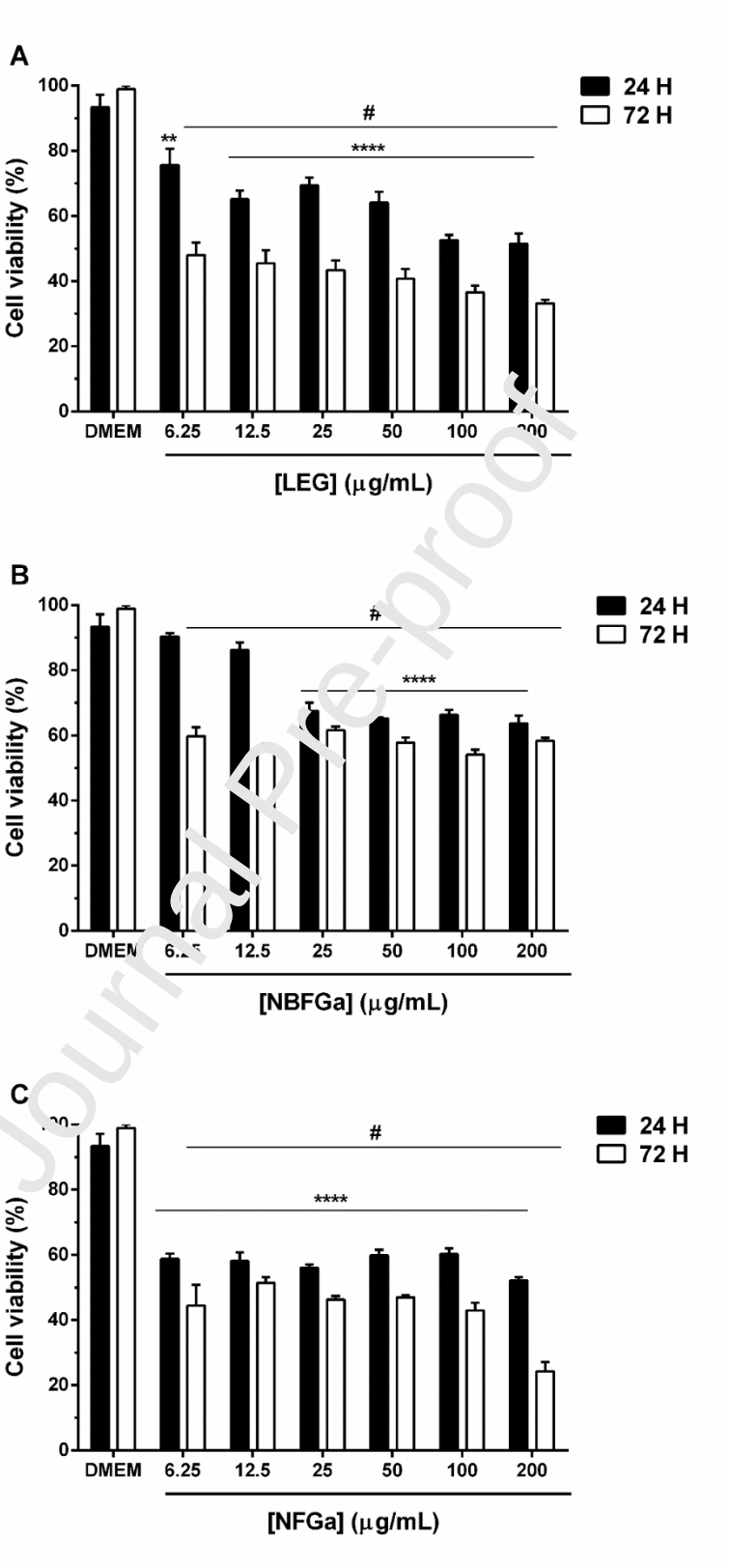

Fig. 8

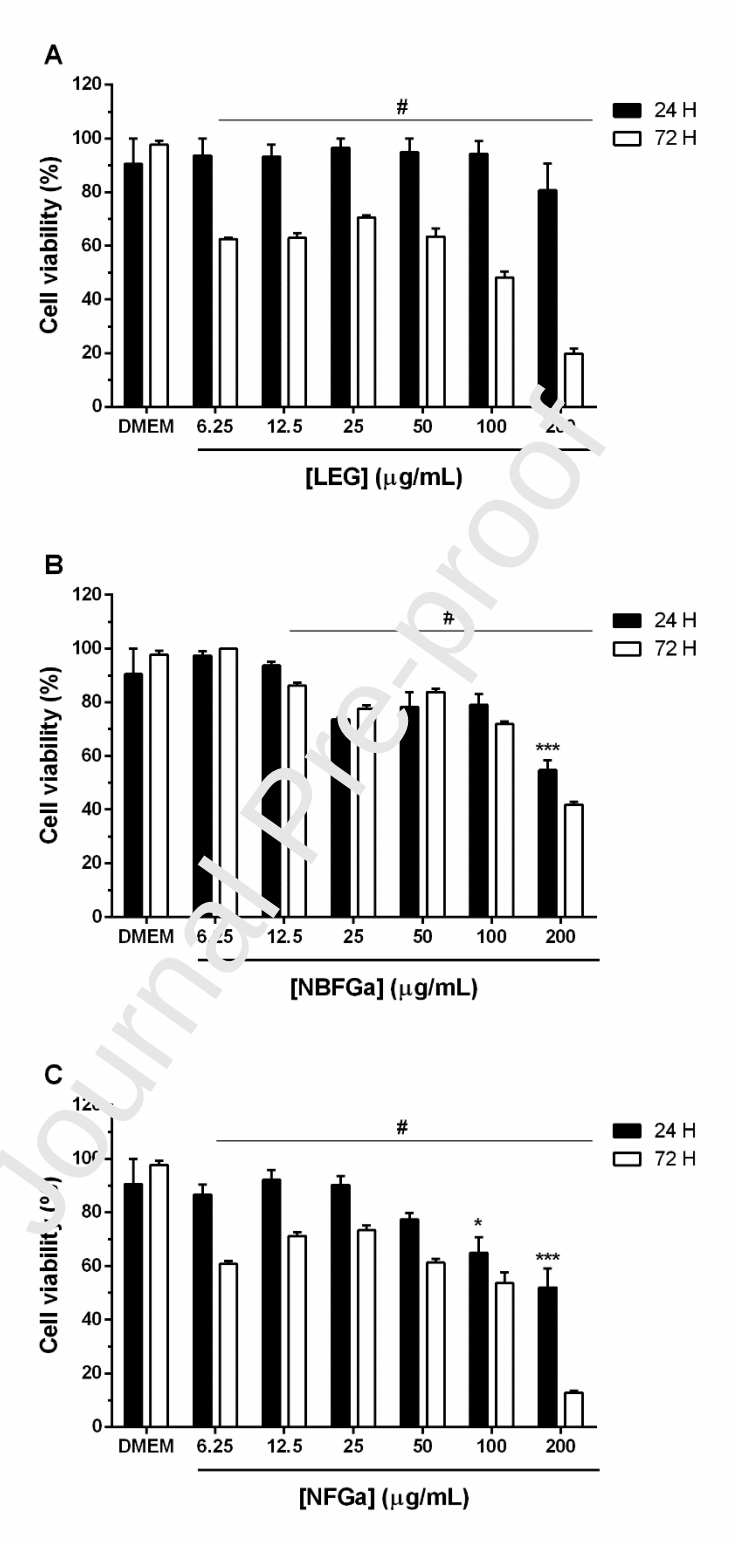

Fig. 9

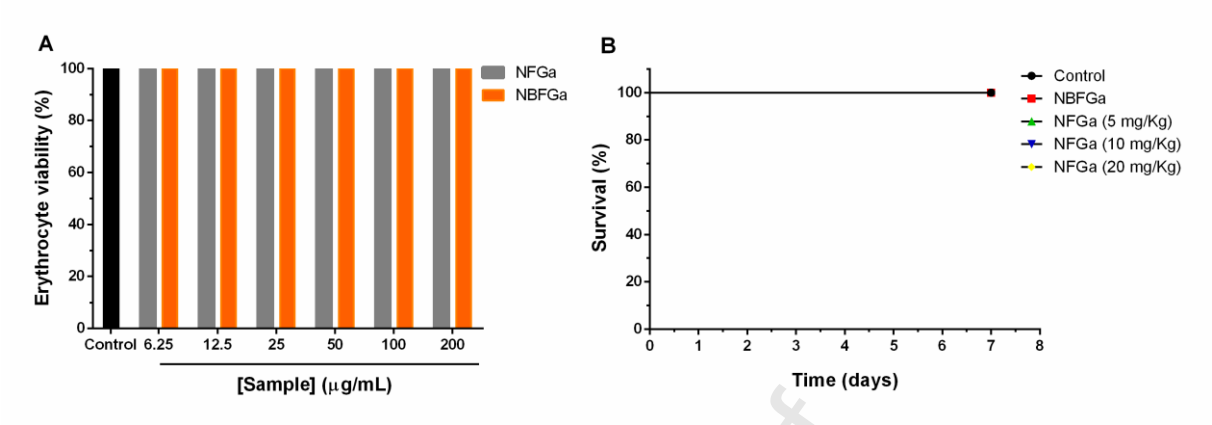

Authorship contributions

Conception and design of study: D. A. Silva, J. R. S. A. Leite, E. O. Andrades.

acquisition of data: E. O. Andrades, J. M. A. R. Costa, F. E. M. Lima Neto, A. R. F. O. S. Ribeiro, A. G. Vasconcelos, A. C. J. Oliveira, M. P. Almeida, J. N. Dias, I. G. M. Silva.

analysis and/or interpretation of data: E. O. Andrades, D. A. Silva, J. R. S. A. Leite, A. R. Araujo, J. L. Soares Sobrinho, A. P. Carvalho, P. Albuquerque, I. S. Pereira, D. A. Rabello, A. G. N. Amorim.

Drafting the manuscript: E. O. Andrades, J. M. A. R. Costa, F. E. M. Lima Neto, A. R. Araujo, F. O. S. Ribeiro, A. G. Vasconcelos.

revising the manuscript critically for important intellectual content: D. A. Silva, J. R. S. A. Leite, E. O. Andrades, A. R. Araujo, A. G. Vasconcelos.

Approval of the version of the manuscript to be published: E. O. Andrades, J. M. A. R. Costa, F. E. M. Lima Neto, A. R. Araujo, F. O. S. Ribeiro, A. G. Vasconcelos, A. C. J. Oliveira, J. L. Soares Sobrinho, M. P. Almeida, A. P. Carvalho, J. N. Dias, I. G. M. Silva, P. Albuquerque, I. S. Pereira, D. A. Rabello, A. G. N. Amorim, J. R. S. A. Leite, D. A. Silva.

Highlights

- Nanocarrier based on fucan-coated acetylated cashew gum containing lycopene-rich extract from red guava was produced.
- The fucan coating improved the encapsulation efficiency and physicochemical properties.
- Lycopene-rich extract encapsulated was more stable than free extract.
- Nanocarriers showed high cytotoxicity against breast cancer cells and low toxicity in normal model.